universe

MDPI

Article

Scale-Dependent Gravity in Quantum Cosmology I: Singularity-Avoiding Sectors and Semiclassical Dynamics

Ibrahim Jarra [1], Rohan Bolle [1], Benjamin R. Furst [2], Justin M. Conroy [2] and Jeffery A. Secrest [1,*]

[1] Department of Biochemistry, Chemistry and Physics, Georgia Southern University, Armstrong Campus, 11935 Abercorn St, Savannah, GA 31419, USA; ij01273@georgiasouthern.edu (I.J.); rohanbolle@gmail.com (R.B.)
[2] Department of Physics, State University of New York at Fredonia, 280 Central Ave, Fredonia, NY 14063, USA; bfurst22@gmail.com (B.R.F.); justin.conroy@fredonia.edu (J.M.C.)
* Correspondence: jsecrest@georgiasouthern.edu

Abstract

We study an effective quantum cosmological model with a scale-dependent gravitational coupling $G(a)$. Starting from a Newtonian cosmological construction inspired by a corrected two-body gravitational potential, we derive an effective Friedmann-type equation and quantize the corresponding minisuperspace model to obtain a Wheeler–DeWitt equation. For the power-law running $G(a) = G_0 a^n$, the small-scale behavior is controlled by the exponent n. In the flat dust model under the repulsive effective-potential prescription adopted here, with a quantum correction term $\Xi > 0$, the values $n = 3/2$ and $n = 2$ mark distinct analytic boundaries: $n = 3/2$ marks the sign change of the quantum-correction coefficient, while $n = 2$ marks the degeneracy of the leading powers of a. A genuine bounce occurs only when a root of $H^2(a)$ separates a forbidden small-a region from an allowed expanding branch, so that nonsingular sectors appear without spatial curvature, exotic matter, or nonstandard quantization prescriptions. We obtain Bessel, Airy, numerical, and WKB solutions, and show that the model separates genuine DeWitt suppression from regularity at the origin. The WKB analysis exhibits a forbidden region, a turning point, and an oscillatory semiclassical branch, while the conserved probability current distinguishes expanding and contracting sectors. A scalar field treated as a weakly backreacting internal clock yields wave packets that track the leading-order classical relational trajectory at a large scale factor; the WKB Hamilton–Jacobi limit recovers the modified Friedmann dynamics as the leading-order phase of the Wheeler–DeWitt wave function.

Keywords: quantum cosmology; Wheeler–DeWitt equation; running gravitational coupling; nonsingular cosmology; cosmological bounce; minisuperspace quantization; DeWitt boundary condition; semiclassical limit

Check for updates

Academic Editors: Gonzalo J. Olmo and Daniele Oriti

Received: 29 June 2026
Revised: 10 September 2026
Accepted: 15 September 2026
Published: 22 September 2026

Copyright: © 2026 by the authors. Licensee MDPI, Basel, Switzerland. This article is an open access article distributed under the terms and conditions of the Creative Commons Attribution (CC BY) license.

1. Introduction

One of the central questions in quantum cosmology concerns whether the initial singularity of the classical Friedmann picture is an unavoidable feature of cosmological evolution, or whether quantum effects are capable of resolving it. In the standard classical treatment, generic matter sources drive the scale factor to zero, where the energy density and spacetime curvature diverge and the classical description breaks down [1,2]. This singular behavior has long served as a principal motivation for developing cosmological models within a quantum gravitational framework [3].

A broad class of quantum cosmological models produces a suppressed small-a regime together with a large-a oscillatory regime, admitting a semiclassical interpretation [4–7]. In many instances, however, this outcome depends on the introduction of spatial curvature, exotic matter components [8], special boundary conditions [4,5], or nonstandard quantization prescriptions [9,10]. Here we ask a narrower question: how does quantum-corrected Newtonian cosmology change when the gravitational coupling itself is allowed to run with the cosmological scale factor?

In this paper, we address this question by studying a cosmological model in which the gravitational coupling depends on the scale factor, $G(a)$ [11], while the remaining cosmological structure is kept as simple as possible. Starting from a quantum-corrected Newtonian cosmology [12,13], we derive a modified Friedmann equation in which the running of the gravitational coupling enters through effective couplings $G^*(a)$, $G_1^{*2}(a)$, and $G_2^{*2}(a)$, defined as the first integrals of the equation of motion. A scale-dependent G does more than rescale the standard Friedmann equation: after the first integral is taken, it changes the effective powers and coefficients that appear in the matter, classical-correction, and quantum-correction terms.

In the power-law case $G(a) = G_0\, a^n$, the small-a behavior is governed entirely by the scaling exponent n, so that the transition between a crunching and a bouncing cosmology is determined by the scaling exponent rather than fine-tuned parameter cancellations. For the flat dust model under the repulsive effective-potential prescription adopted here, with $\Xi > 0$, the values $n = 3/2$ and $n = 2$ mark distinct analytic boundaries. A genuine bounce occurs only when the root of $H^2(a)$ separates a forbidden small-a region from an allowed large-a branch. The global fate of the universe is therefore controlled by the scaling behavior of gravity itself, without modification of the matter content or spatial geometry.

We construct an effective minisuperspace quantization of this model [14], leading to a Wheeler–DeWitt-type equation [3]. It should be noted that there are longstanding questions regarding this approach toward Wheeler–Dewitt cosmology, including factor ordering, the problem of time, the physical Hilbert space, and its relation to a more fundamental theory of quantum gravity. This paper does not claim to resolve these issues, but rather examines a phenomenological model within the Wheeler–DeWitt minisuperspace framework, with its assumptions and limitations stated explicitly. For selected parameter choices, the theory admits exact analytic solutions of both Bessel and Airy type, as well as numerical solutions in physically relevant cases [15]. Recently, model-specific and nonstandard realizations of the Wheeler–DeWitt equation have appeared in the literature [16]. These solutions demonstrate that the wave function can be strongly suppressed near $a = 0$, satisfying the DeWitt boundary condition [3] and indicating singularity avoidance, while in other sectors the wave function remains regular but nonvanishing at the origin [4]. The model therefore separates two cases that should not be conflated: a wave function that vanishes at $a = 0$, and a wave function that is regular but nonzero there.

We also carry out a WKB analysis and show that, for appropriate parameter choices, the wave function exhibits the structure of a nonsingular quantum cosmology: a classically forbidden region at a small scale factor, a turning point, and an oscillatory semiclassical regime at a large scale factor. The conserved minisuperspace probability current provides a means to distinguish expanding and contracting branches, giving the oscillatory wave function a dynamical interpretation. Finally, we introduce a homogeneous scalar field as an internal clock [17], which allows wave packets to be constructed and followed in relational time. In the case studied here, and within the weak-backreaction test-field regime, the packet peak tracks the leading-order classical relational trajectory at a large scale factor.

The paper is organized as follows. In Section 2, we derive the modified Friedmann equation for a running gravitational coupling and define the effective couplings that

control the dynamics. In Section 3, we quantize the model and present exact solutions of the Wheeler–DeWitt equation. In Section 4, we develop the WKB analysis and probability-current interpretation. In Section 5, we introduce the scalar-field clock and examine the quantum-to-classical correspondence in relational time. The final sections summarize the physical implications of the model.

2. Quantum-Corrected Newtonian Cosmology

2.1. Newtonian Cosmological Setup

We begin with the standard Newtonian cosmology construction. Assuming homogeneity and isotropy, consider a test particle of negligible mass located on the boundary of a spherical region of physical radius $R(t)$, filled with a uniform mass density $\rho(t)$. By symmetry, only the mass enclosed within radius R contributes to the gravitational force on the particle.

The physical radius of the shell is written as

$$R(t) = a(t)R_0, \tag{1}$$

where $a(t)$ is the cosmological scale factor and R_0 is a comoving coordinate label identifying the shell. The quantity R_0 is not observable and reflects a freedom in the normalization of comoving coordinates. The enclosed mass is

$$M(R) = \frac{4\pi}{3} R^3 \rho(t), \tag{2}$$

and the Hubble parameter is defined kinematically as

$$H(t) \equiv \frac{\dot{a}}{a} = \frac{\dot{R}}{R}. \tag{3}$$

We assume that the cosmic fluid obeys a barotropic equation of state,

$$p = (\gamma - 1)\rho c^2, \tag{4}$$

which implies, through the continuity equation,

$$\rho(t) = \rho_0 a^{-3\gamma}, \tag{5}$$

where ρ_0 denotes the density at the present epoch.

2.2. Quantum-Corrected Newtonian Force Law

To incorporate classical and quantum corrections to Newtonian gravity, we adopt an effective radial force law motivated by quantum corrections to the gravitational potential [12,13,18–20]. The acceleration of the test particle is taken to be

$$\ddot{R} = -\frac{G(R)M}{R^2} - 2\lambda \frac{G(R)^2 M^2}{c^2 R^3} + 3\xi_{\mathrm{QG}} \frac{\hbar G(R)^2 M}{c^3 R^4}. \tag{6}$$

The first term is the standard Newtonian attraction, the second is the leading classical correction, and the third is the leading quantum correction proportional to $\hbar$. In the sign convention adopted here, $\xi_{\mathrm{QG}} > 0$ denotes the magnitude of the repulsive quantum correction. The parameters λ and ξ_{QG} encode the relative strengths of the higher-order classical and quantum contributions.

In the present work we allow the gravitational coupling to depend on scale. Thus, G is not treated as a fixed constant, but as a function of the cosmological scale through

$G = G(R)$, or equivalently, $G = G(a)$. In Equation (6), we adopt the corrected force law first and then promote G to $G(R)$. We do not insert $G(R)$ into the two-body potential and differentiate it afterward; that alternative prescription would produce additional dG/dR terms. The effects of the running in our model enter through the first integral and the effective couplings defined below.

2.3. First Integral of the Equation of Motion

When G varies with scale, the force is not strictly conservative in the ordinary Newtonian sense, and a conserved mechanical energy should not be assumed at the outset. Instead, a first integral can be obtained from Newton's second law. Multiplying Equation (6) by $\dot{R}$ and integrating with respect to time gives

$$\int \ddot{R}\,\dot{R}\,dt = \int f(R,G)\,dR, \tag{7}$$

where $f(R,G)$ denotes the right-hand side of Equation (6). Integration gives

$$\begin{aligned}\frac{1}{2}\dot{R}^2 = \frac{M}{R}\left[G - R\int \frac{dG}{R}\right] + \lambda\,\frac{M^2}{c^2R^2}\left[G^2 - 2R^2\int \frac{G}{R^2}\,dG\right] \\ - \xi_{\mathrm{QG}}\,\frac{M\hbar}{c^3R^3}\left[G^2 - 2R^3\int \frac{G}{R^3}\,dG\right] + C,\end{aligned} \tag{8}$$

where C is an integration constant.

It is convenient to define the effective gravitational couplings

$$G^* \equiv G - R\int \frac{dG}{R}, \tag{9}$$

$$G_1^{*2} \equiv G^2 - 2R^2\int \frac{G}{R^2}\,dG, \tag{10}$$

$$G_2^{*2} \equiv G^2 - 2R^3\int \frac{G}{R^3}\,dG. \tag{11}$$

In terms of these quantities, Equation (8) becomes

$$\frac{1}{2}\dot{R}^2 = \frac{G^*M}{R} + \lambda\,\frac{G_1^{*2}M^2}{c^2R^2} - \xi_{\mathrm{QG}}\,\frac{\hbar G_2^{*2}M}{c^3R^3} + C. \tag{12}$$

The constant C is the Newtonian integration constant and will be identified with the spatial curvature term. The quantities G^*, G_1^{*2}, and G_2^{*2} are not new independent constants. They are effective couplings generated by the scale dependence of G. In the constant-G limit, the integral contributions vanish and the usual Newtonian/Friedmann structure is recovered. For a genuinely running coupling, however, the starred quantities need not scale in the same way as $G(R)$ itself. They therefore summarize how the running of gravity modifies the matter, classical-correction, and quantum-correction sectors of the cosmological dynamics.

2.4. Friedmann-Type Equation

Dividing Equation (12) by R^2 and using $H = \dot{R}/R$, we find

$$H^2 = \frac{2G^*M}{R^3} + \lambda\,\frac{2G_1^{*2}M^2}{c^2R^4} - \xi_{\mathrm{QG}}\,\frac{2\hbar G_2^{*2}M}{c^3R^5} + \frac{2C}{R^2}. \tag{13}$$

Substituting

$$M = \frac{4\pi}{3} R^3 \rho \tag{14}$$

gives

$$H^2 = \frac{8\pi}{3} G^* \rho + \lambda \frac{32\pi^2}{9c^2} G_1^{*2} R^2 \rho^2 - \xi_{\mathrm{QG}} \frac{8\pi}{3} \frac{\hbar}{c^3} G_2^{*2} \frac{\rho}{R^2} + \frac{2C}{R^2}. \tag{15}$$

Using $R = aR_0$, the last term becomes

$$\frac{2C}{R^2} = \frac{2C}{a^2 R_0^2}. \tag{16}$$

We identify the curvature parameter by

$$k \equiv -\frac{2C}{c^2 R_0^2}, \tag{17}$$

so that

$$\frac{2C}{R^2} = -\frac{kc^2}{a^2}. \tag{18}$$

The higher-order terms retain a dependence on the reference scale R_0. We collect this dependence into the effective coefficients $\mathrm{Y_{cl}}$ and Ξ:

$$\mathrm{Y_{cl}} \equiv \lambda R_0^2, \qquad \Xi \equiv \frac{\xi_{\mathrm{QG}}}{R_0^2}. \tag{19}$$

Here, ξ_{QG} is the dimensionless coefficient of the one-loop quantum correction to the Newtonian potential, whereas Ξ is the corresponding dimensionful coefficient entering the cosmological equation. Thus,

$$[\xi_{\mathrm{QG}}] = 1, \qquad [\Xi] = L^{-2}.$$

Substituting $\rho = \rho_0 a^{-3\gamma}$, the effective Friedmann-type equation inspired by the corrected Newtonian potential becomes

$$\begin{aligned} H^2(a) = {} & \frac{8\pi}{3} G^*(a) \rho_0 a^{-3\gamma} + \mathrm{Y_{cl}} \frac{32\pi^2}{9c^2} G_1^{*2}(a) \rho_0^2 a^{2-6\gamma} \\ & - \Xi \frac{8\pi}{3} \frac{\hbar}{c^3} G_2^{*2}(a) \rho_0 a^{-(3\gamma+2)} - \frac{kc^2}{a^2}. \end{aligned} \tag{20}$$

This is the basic dynamical equation used throughout the remainder of the paper. It reduces to the standard Friedmann equation when the higher-order corrections are removed and $G^* \to G_0$. At a small scale factor, however, the correction terms can become significant and may alter the approach to the classical singularity.

2.5. Normalized Density Formulation

It is often convenient to rewrite Equation (20) in terms of dimensionless density parameters. We introduce the present-day critical density

$$\rho_{c,0} \equiv \frac{3H_0^2}{8\pi G_0}, \tag{21}$$

where H_0 and G_0 are the present values of the Hubble parameter and gravitational coupling, respectively. The corresponding density parameter is

$$\Omega_0 \equiv \frac{\rho_0}{\rho_{c,0}} = \frac{8\pi G_0 \rho_0}{3H_0^2}. \tag{22}$$

Thus,

$$\frac{8\pi}{3}\rho_0 = \frac{\Omega_0 H_0^2}{G_0}, \tag{23}$$

$$\frac{32\pi^2}{9}\rho_0^2 = \frac{\Omega_0^2 H_0^4}{2G_0^2}. \tag{24}$$

Substitution into Equation (20) gives

$$\begin{aligned} H^2(a) = &\left(\frac{\Omega_0 H_0^2}{G_0}\right) G^*(a) a^{-3\gamma} + \Upsilon_{\rm cl}\left(\frac{\Omega_0^2 H_0^4}{2G_0^2 c^2}\right) G_1^{*2}(a) a^{2-6\gamma} \\ &- \Xi\left(\frac{\Omega_0 H_0^2}{G_0}\right)\frac{\hbar}{c^3} G_2^{*2}(a) a^{-(3\gamma+2)} - \frac{kc^2}{a^2}. \end{aligned} \tag{25}$$

Dividing by H_0^2, one obtains the form

$$\begin{aligned} \frac{H^2(a)}{H_0^2} = &\Omega_0 \frac{G^*(a)}{G_0} a^{-3\gamma} + \Upsilon_{\rm cl}\Omega_0^2 \frac{H_0^2}{2G_0^2 c^2} G_1^{*2}(a) a^{2-6\gamma} \\ &- \Xi\Omega_0 \frac{\hbar}{G_0 c^3} G_2^{*2}(a) a^{-(3\gamma+2)} - \frac{kc^2}{a^2 H_0^2}. \end{aligned} \tag{26}$$

This form is especially advantageous for numerical work, because the cosmological evolution is expressed in terms of the density parameters and the scale-dependent effective couplings.

2.6. Worked Examples and Physical Interpretation

To illustrate the physical meaning of Equation (20), we now consider two simple examples in order to show how the higher-order correction terms can change the small-scale dynamics even in a homogeneous and isotropic Newtonian cosmology.

Throughout this subsection, we restrict attention to dust matter, $\gamma = 1$, and spatial flatness, $k = 0$, so that the effects of the classical and quantum corrections can be isolated.

2.6.1. Constant Gravitational Coupling

First consider the constant-G limit,

$$G(a) = G_0. \tag{27}$$

Then

$$G^*(a) = G_0, \qquad G_1^{*2}(a) = G_0^2, \qquad G_2^{*2}(a) = G_0^2. \tag{28}$$

For dust and flat geometry, Equation (20) reduces to

$$H^2(a) = \mathcal{A}a^{-3} + \mathcal{B}a^{-4} - \mathcal{C}a^{-5}, \tag{29}$$

where

$$\mathcal{A} \equiv \frac{8\pi}{3} G_0 \rho_0, \tag{30}$$

$$\mathcal{B} \equiv \Upsilon_{\rm cl} \frac{32\pi^2}{9c^2} G_0^2 \rho_0^2, \tag{31}$$

$$\mathcal{C} \equiv \Xi \frac{8\pi}{3} \frac{\hbar}{c^3} G_0^2 \rho_0. \tag{32}$$

As $a \to 0$, the ordinary dust contribution diverges as a^{-3}, the classical correction as a^{-4}, and the quantum correction as a^{-5}. Thus, the quantum term is the most singular contribution in the constant-G case.

A bounce occurs when H^2 vanishes at a finite nonzero scale factor a_b, with a forbidden region at smaller a. From Equation (29), the condition $H^2(a_b) = 0$ gives

$$\mathcal{A} a_b^2 + \mathcal{B} a_b - \mathcal{C} = 0. \tag{33}$$

The physically relevant root is

$$a_b = \frac{-\mathcal{B} + \sqrt{\mathcal{B}^2 + 4\mathcal{A}\mathcal{C}}}{2\mathcal{A}}. \tag{34}$$

Within the truncated phenomenological equation, this root corresponds to a nonsingular bounce [13,21]. Because the quantum correction is derived as a low-energy, long-distance expansion, this result should be regarded as a formal property of the effective model rather than as a controlled prediction at arbitrarily small scales.

2.6.2. Power-Law Running of the Gravitational Coupling

We now consider the scale-dependent ansatz

$$G(a) = G_0 \, a^n. \tag{35}$$

This power law is simple enough to be solved in closed-form while capturing the effect of a running gravitational coupling [22,23]. Using Equations (10)–(12), one finds

$$G^*(a) = \frac{G_0}{1-n} a^n, \qquad G_1^{*2}(a) = \frac{G_0^2}{1-n} a^{2n}, \qquad G_2^{*2}(a) = -\frac{3G_0^2}{2n-3} a^{2n}, \tag{36}$$

valid for $n \neq 1$ and $n \neq 3/2$. Substituting into Equation (26) gives

$$\frac{H^2(a)}{H_0^2} = \frac{\Omega_0}{1-n} a^{n-3} + \Upsilon_{\rm cl} \, \Omega_0^2 \frac{H_0^2}{2c^2(1-n)} a^{2n-4} + 3\,\Xi\,\Omega_0 \frac{\hbar G_0}{c^3} \frac{1}{2n-3} a^{2n-5} - \frac{kc^2}{a^2 H_0^2}. \tag{37}$$

This expression shows why the exponent n controls the small-a behavior of the effective Friedmann equation rather than rescaling it. For dust, the matter, classical-correction, and quantum-correction terms scale as

$$a^{n-3}, \qquad a^{2n-4}, \qquad a^{2n-5},$$

respectively. Two exponents fix the small-scale structure. The quantum term is the most singular contribution whenever

$$2n - 5 < n - 3 \quad \Longrightarrow \quad n < 2, \tag{38}$$

while the coefficient of the quantum contribution changes sign at

$$n = \tfrac{3}{2}. \tag{39}$$

The values $n = 3/2$ and $n = 2$ therefore mark the natural analytic boundaries of the small-scale dynamics: the former is the sign change of the quantum-correction coefficient, while the latter is the power-degeneracy at which the matter and quantum terms scale with the same power of a.

For the simplified flat model with $\Upsilon_{\rm cl} = 0$, the relevant two-term equation is

$$\frac{H^2(a)}{H_0^2} = \frac{\Omega_0}{1-n}\, a^{n-3} + 3\,\Xi\,\Omega_0\, \frac{\hbar G_0}{c^3}\, \frac{1}{2n-3}\, a^{2n-5}. \tag{40}$$

These two boundaries divide the equation into physically distinct regimes, and it is essential to keep separate two questions that are easily conflated: which term dominates the small-a behavior, and whether that behavior corresponds to a bounce.

In the interval

$$\tfrac{3}{2} < n < 2, \tag{41}$$

the quantum term is the most singular contribution and therefore controls the small-a dynamics. Its coefficient is positive throughout this window, since $2n - 3 > 0$, while the running renders the matter coefficient negative, since $1 - n < 0$. The dominant small-a term is thus positive, so $H^2(a) > 0$ as $a \to 0$, and the small-scale region remains classically *allowed*. Any root of $H^2(a)$ in this interval is consequently an upper turning point, or recollapse scale, rather than a singularity-avoiding bounce. Dominance of the quantum correction is not, by itself, a bounce.

A genuine bounce requires the opposite sign structure. For $n > 2$, the matter term becomes the most singular contribution, and because the running carries the factor $1/(1-n)$, its coefficient is negative; the small-a region is then classically *forbidden*, with $H^2(a) < 0$, while the quantum term dominates at larger a and restores an allowed expanding branch. The root that separates these regions is a true bounce. The boundary case $n = 2$ is degenerate: both terms scale with the same power of a, so no isolated turning point exists, and the bounce branch opens up only for $n > 2$.

This distinction is applied in the numerical survey below, where a root of $H^2(a)$ is classified as a bounce only when it separates a forbidden small-a region from an allowed expanding branch. The condition $H^2(a_b) = 0$ alone is not sufficient: a bounce requires both the vanishing of H^2 and the correct sign structure of $H^2(a)$ on the two sides of the root.

The small-a behavior is therefore controlled by the scaling behavior of gravity itself. The dominance of the quantum term as $a \to 0$ is an algebraic statement about the truncated modified Friedmann equation and should not be interpreted as establishing the validity of the underlying one-loop potential at arbitrarily small scales. The quantum correction is derived as a long-distance, low-energy effective-field-theory expansion. Its local expansion parameter is

$$\epsilon_{\rm Q}(a) \equiv \xi_{\rm QG} \frac{\hbar G(a)}{c^3 R(a)^2}. \tag{42}$$

For $G(a) = G_0 a^n$ and $R(a) = aR_0$, this becomes

$$\epsilon_{\rm Q}(a) = \zeta a^{n-2}, \tag{43}$$

where $\zeta = \hbar G_0 \xi_{\rm QG}/(c^3 R_0^2)$. Perturbative control of the one-loop potential requires $\epsilon_{\rm Q} \ll 1$, together with the usual post-Newtonian condition $G(a)M/[R(a)c^2] \ll 1$. For $n < 2$, $\epsilon_{\rm Q}$ diverges as $a \to 0$, whereas for $n > 2$, it decreases toward the origin. The turning-point

solutions considered below must nevertheless be checked at the finite value $a = a_t$, rather than only through their asymptotic scaling.

Even with dust matter and flat spatial geometry, a running gravitational coupling can make the effective Friedmann equation behave like a multi-fluid system, and the transition between recollapsing and bouncing behavior can be achieved by the power-law form of $G(a)$, without the need to add exotic matter by hand.

The quantum-correction parameter used below is inherited from the effective two-body potential adopted in the present phenomenological construction. Earlier calculations of the leading quantum correction to the Newtonian potential produced different coefficients and signs, reflecting differences in the definition of the potential and in the treatment of the scattering amplitude and iterated contributions [13,18]. Here we follow the effective-potential prescription of Hamber and Liu [18], for which the correction is repulsive in the force-law convention of Equation (6), and write

$$V(r) = -\frac{GM}{r}\left[1 + \frac{3G(M+m)}{rc^2} - \xi_{\mathrm{QG}}\frac{\hbar G}{r^2c^3} + \cdots\right], \tag{44}$$

where the coefficient multiplying the one-loop quantum correction is

$$\xi_{\mathrm{QG}} = \frac{122}{15\pi}. \tag{45}$$

With the convention of Equation (44), the quantum part of the potential per unit test mass is

$$V_{\mathrm{Q}}(r) = +\xi_{\mathrm{QG}}\frac{\hbar G^2 M}{c^3 r^3}. \tag{46}$$

Its radial contribution to the acceleration is therefore

$$a_{\mathrm{Q}}(r) = -\frac{dV_{\mathrm{Q}}}{dr} = +3\xi_{\mathrm{QG}}\frac{\hbar G^2 M}{c^3 r^4}, \tag{47}$$

which agrees with the sign of the quantum term in Equation (6).

The coefficient and sign of a quantum correction to a coordinate-space gravitational potential have not been presented uniformly in the literature. In particular, the Hamber–Liu prescription adopted here yields the repulsive correction written above, whereas the later effective-field-theory result of Bjerrum-Bohr, Donoghue, and Holstein, including its erratum, gives the commonly quoted coefficient $41/(10\pi)$ with the opposite force sign in the present convention [24–26]. Because the coordinate-space potential is prescription-dependent, the resulting cosmological correction should be understood as a phenomenological input rather than as a prescription-independent prediction of low-energy quantum gravity. The singularity-avoiding sectors studied below are therefore conditional on the repulsive Hamber–Liu prescription.

The coefficient ξ_{QG} is dimensionless. The quantity entering the cosmological modified Friedmann equation is instead

$$\Xi \equiv \frac{\xi_{\mathrm{QG}}}{R_0^2}, \tag{48}$$

and therefore has dimensions $[\Xi] = L^{-2}$. For normalized parameter surveys, the relevant dimensionless combination is

$$\zeta \equiv \frac{\hbar G_0}{c^3}\Xi = \frac{\hbar G_0}{c^3 R_0^2}\xi_{\mathrm{QG}}. \tag{49}$$

Within the Hamber–Liu prescription adopted here, the dimensionless microscopic coefficient has the magnitude $\xi_{\mathrm{QG}} = 122/(15\pi)$. The effective cosmological coefficient

$\Xi = \xi_{QG}/R_0^2$ is dimensionful, while $\zeta = \hbar G_0 \Xi / c^3$ is dimensionless and is the parameter that appears in the normalized modified Friedmann equation. Its numerical value also depends on the reference scale R_0. The value of ζ shifts the location of a turning point, whereas the existence and classification of the turning point are controlled primarily by the scaling exponent n.

We emphasize that the coefficient ξ_{QG} was derived for the static, two-body gravitational potential in asymptotically flat spacetime, and its use here—via the Newtonian shell construction of Sections 2.1–2.4—to correct a homogeneous, cosmological background is a phenomenological ansatz rather than a first-principles covariant derivation. A manifestly covariant treatment of one-loop quantum-gravitational corrections to FRW cosmology would instead organize the corrections in the gravitational effective action as local curvature-squared invariants (e.g., $c_1 R^2 + c_2 R_{\mu\nu} R^{\mu\nu}$) together with nonlocal form-factor terms [27–29], rather than as a term inherited from the static two-body force law. Interestingly, our classical-correction term Y_{cl}, which enters $H^2(a)$ as ρ^2, has a scaling that is qualitatively reminiscent of a curvature-squared correction in FRW, since $\rho^2 \sim H^4$ at the level of Friedmann scaling. The Ξ term does not have an equally direct covariant pedigree, and its translation into a cosmological setting rests on the Newtonian construction alone. Establishing the precise relation between the power-law ansatz used here and the powers of a generated by a genuinely covariant curvature expansion—which are generically different from, and plausibly more singular than, those obtained from the two-body potential—is left for future work.

2.7. Possible Origins of Scale-Dependent Power-Law Running

The ansatz

$$G(a) = G_0 a^n \tag{50}$$

is phenomenological, but power-law behavior can arise in several extensions of gravity. In asymptotically safe quantum gravity, the running Newton coupling near an ultraviolet fixed point behaves as $G(k) \sim k^{-2}$. Under an appropriate cosmological identification of the renormalization-group scale, such as $k \propto a^{-1}$, this gives $G(a) \sim a^2$ [30,31]. In scalar–tensor theories, a coupling function of the form $F(\phi) \sim e^{\alpha\phi}$ can generate an effective power law in a when the scalar field evolves logarithmically with the scale factor [32]. Kaluza–Klein compactifications with a time-dependent modulus can likewise produce a scale-dependent four-dimensional gravitational coupling [33]. We do not derive the form of $G(a)$ from any of these frameworks here. They are cited only as examples in which power-law running may arise as an effective scaling regime.

The strict power law is analytically tractable and is used throughout this paper as a local description of the deep-ultraviolet regime $a \to 0$. It cannot, however, persist unchanged throughout the later universe. Compatibility with primordial nucleosynthesis, recombination, structure formation, and local limits on $\dot{G}/G$ requires the running to freeze out before the relevant observational epochs.

A smooth interpolation that preserves the normalization of the early-time power law may be written as

$$G(a) = G_0 \left[a^n + (1 - a^n) \exp\left(-\left(\frac{a_x}{a} \right)^p \right) \right], \qquad p > n > 0, \tag{51}$$

where a_x sets the transition scale and p controls the sharpness of the transition. This profile is introduced only as an illustrative global completion of the local power-law model.

In the deep-ultraviolet limit, $a \ll a_x$, the exponential term is suppressed faster than any finite power of a, and therefore

$$G(a) = G_0 a^n + \mathcal{O}\left[\exp\left(-\left(\frac{a_x}{a}\right)^p\right)\right]. \tag{52}$$

Thus,

$$G(a) \simeq G_0 a^n, \qquad a \to 0, \tag{53}$$

with precisely the same normalization used in the pure power-law analysis. In particular, no additional factor proportional to a_x^{-n} is introduced.

For $a \gg a_x$, one may expand

$$\exp\left(-\left(\frac{a_x}{a}\right)^p\right) = 1 - \left(\frac{a_x}{a}\right)^p + \mathcal{O}\left[\left(\frac{a_x}{a}\right)^{2p}\right]. \tag{54}$$

Equation (51) then gives

$$\frac{G(a)}{G_0} = 1 - (1 - a^n)\left(\frac{a_x}{a}\right)^p + \mathcal{O}\left[\left(\frac{a_x}{a}\right)^{2p}\right]. \tag{55}$$

The condition $p > n$ ensures that the residual correction decreases in the late-time regime, so that

$$G(a) \longrightarrow G_0. \tag{56}$$

For the turning points examined in Section 2.8, the relevant dynamics occur in the early-time regime in which the pure power law is applicable. The transition scale a_x must nevertheless be chosen so that the running becomes observationally negligible before the BBN epoch, $a_{\rm BBN} \sim 10^{-10}$. More precisely, both a_x and the sharpness parameter p must be constrained so that $|G(a)/G_0 - 1|$ and $|\dot{G}/G|$ satisfy the relevant bounds during BBN and subsequent cosmological epochs. We do not perform that global parameter analysis here.

Accordingly, the calculations in this paper use $G(a) = G_0 a^n$ as a local early-universe scaling model rather than as a complete description of gravity at all epochs. A full phenomenological analysis would require specifying the transition parameters and comparing the resulting history of $G(a)$ with cosmological and local constraints. The observational consequences of allowing the running to persist into the BBN era, recombination, and the epoch of structure formation are considered in Ref. [34].

2.8. Bounce-Scale Parameter Survey

The power-law model also allows a simple analytic and numerical survey of the turning-point scale. To isolate the role of the running exponent, we consider the dust, flat, and purely quantum-corrected case,

$$\gamma = 1, \qquad k = 0, \qquad \Upsilon_{\rm cl} = 0,$$

with

$$G(a) = G_0 a^n.$$

In this limit, the effective Friedmann equation reduces to

$$\begin{aligned} \frac{H^2(a)}{H_0^2} &= \frac{\Omega_0}{1-n} a^{n-3} + 3\Xi\Omega_0 \frac{\hbar G_0}{c^3} \frac{1}{2n-3} a^{2n-5}, \\ &= \frac{\Omega_0}{1-n} a^{n-3} + \frac{3\zeta\Omega_0}{2n-3} a^{2n-5}. \end{aligned} \tag{57}$$

For the dimensionless survey shown in Figure 1, the quantum correction is controlled by the combination ζ defined in Equation (49). We choose the reference value

$$\zeta_0 = \frac{122}{15\pi} \tag{58}$$

as an illustrative normalization. This choice corresponds to fixing the reference scale so that $\hbar G_0/(c^3 R_0^2) = 1$. It should not be interpreted as a direct observational determination of R_0 or of the bounce scale.

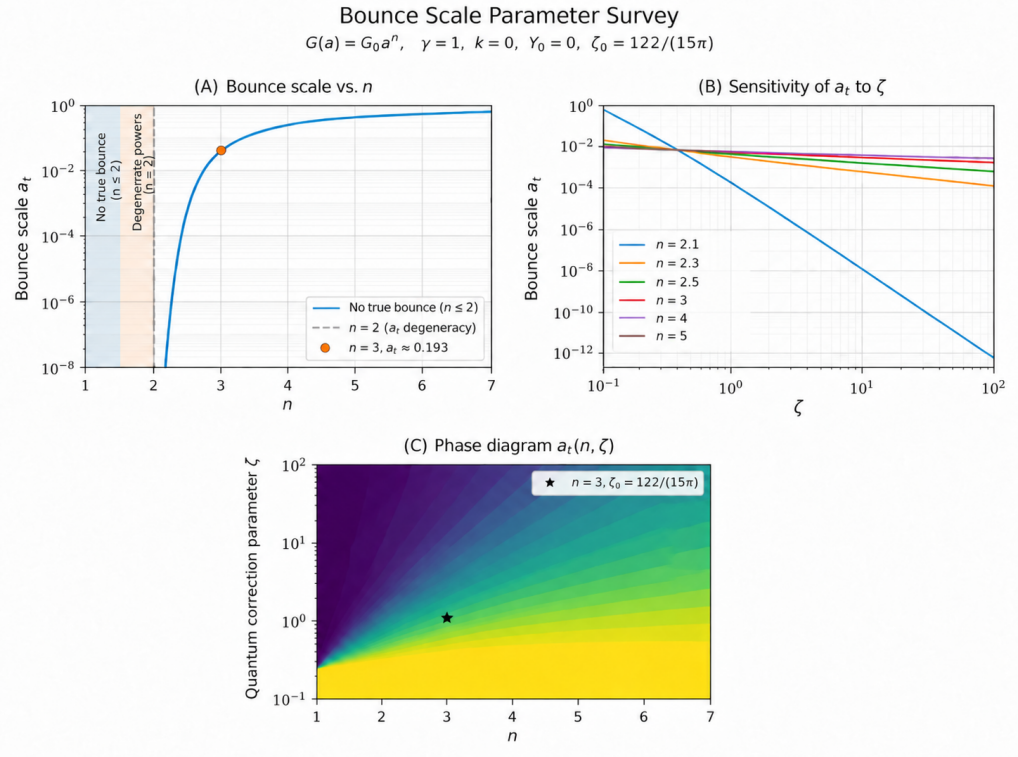


Figure 1. Bounce-scale survey for the power-law running model $G(a) = G_0 a^n$, shown for dust matter ($\gamma = 1$), flat spatial geometry ($k = 0$), and vanishing classical correction ($Y_{\rm cl} = 0$). The survey is expressed in terms of the dimensionless quantum-correction parameter $\zeta = \hbar G_0 \Xi/c^3$. We use the illustrative normalization $\zeta_0 = 122/(15\pi)$, corresponding to $\hbar G_0/(c^3 R_0^2) = 1$. Panel (**A**) shows the true bounce scale a_t as a function of the running exponent n. The shaded region indicates parameter values for which no true bounce occurs, even though a formal turning point may exist. The vertical line at $n = 2$ marks the degenerate case in which the relevant terms scale with the same power of a, and the marked point shows the representative value $n = 3$, for which $a_t \simeq 0.193$. Panel (**B**) shows that the dependence on ζ is highly sensitive near the degenerate value $n = 2$, but becomes much milder for larger n. Panel (**C**) displays the same information as a phase diagram in the (n, ζ) plane, with contours of constant bounce scale.

A turning point occurs when $H^2(a_t) = 0$. From Equation (57), this gives

$$a_t(n, \zeta) = \left[\frac{2n-3}{3\zeta(n-1)}\right]^{1/(n-2)}, \qquad n \neq 1, \frac{3}{2}, 2. \tag{59}$$

For the two-term dust model, Equation (59) implies

$$a_t^{n-2} = \frac{2n-3}{3\zeta(n-1)}. \tag{60}$$

Consequently, the quantum expansion parameter evaluated at the turning point is

$$\epsilon_{\mathrm{Q}}(a_t) = \zeta a_t^{n-2} = \frac{2n-3}{3(n-1)}. \tag{61}$$

For the representative choice $n = 3$, one finds $\epsilon_{\mathrm{Q}}(a_t) = 1/2$. The leading quantum term is therefore not parametrically small at the turning point. We accordingly interpret the bounce as a feature of the phenomenological truncated model, rather than as a quantitatively controlled prediction of low-energy effective field theory.

A root a_t of $H^2(a_t) = 0$ can be of three types:

- **Type I (Bounce):** $H^2(a) < 0$ for $a < a_t$ (forbidden), $H^2(a) > 0$ for $a > a_t$ (allowed). The universe contracts, stops, and re-expands.
- **Type II (Recollapse):** $H^2(a) > 0$ for $a < a_t$, $H^2(a) < 0$ for $a > a_t$. The universe expands, stops, and contracts.
- **Type III (Degenerate):** No sign change across a_t.

Only Type I corresponds to a nonsingular bounce that replaces the classical singularity.

However, not every turning point is a true bounce. A bounce requires more than $H^2(a_t) = 0$: the region $a < a_t$ must be classically forbidden, while the region $a > a_t$ must be classically allowed. In other words, the root must separate an inaccessible small-scale region from an expanding cosmological branch.

For $3/2 < n < 2$, the equation may possess a positive root, but the small-a region remains allowed. Such a solution is better interpreted as an upper turning point or recollapse scale, not as a singularity-avoiding bounce. By contrast, for $n > 2$, the leading small-a behavior makes $H^2(a) < 0$ near the origin, while the larger-a branch becomes allowed. Thus, in the parameter range emphasized here, the true bounce branch begins at $n = 2$. The point $n = 2$ itself is degenerate because the two terms in Equation (57) scale with the same power of a, so there is no isolated turning point.

Figure 1 summarizes the structure of the bounce branch. Figure 1A shows that, for the reference value $\zeta_0 = 122/(15\pi)$, the true bounce scale grows from very small values just above $n = 2$ and approaches order unity as n becomes large. For example, at $n = 3$,

$$a_t = \frac{1}{2\zeta_0} \simeq 0.193. \tag{62}$$

Figure 1B shows that the dependence on ζ is highly sensitive near the degenerate value $n = 2$, but becomes much milder for larger n. Figure 1C displays the same information as a phase diagram in the (n, ζ) plane.

The existence and location of the bounce are controlled primarily by the scaling exponent n. The dimensionless parameter ζ shifts the location of the bounce, but the qualitative transition between a true bounce and a non-bouncing solution is governed by the power-law behavior of the gravitational coupling itself.

2.9. Connection to the Wheeler–DeWitt Analysis

The effective Friedmann equation derived in this section provides the starting point for the minisuperspace quantization in Section 3. In the quantum theory, the same scale dependence of $G(a)$ enters the Wheeler–DeWitt equation through the effective minisuperspace potential. Consequently, the classical turning-point structure and the quantum behavior of the wave function near $a = 0$ are governed by the same underlying running of the gravitational coupling.

Both descriptions inherit the same scale dependence from our effective model. At the classical level, the effective Friedmann-type equation determines whether a solution

reaches $a = 0$, encounters a turning point, or undergoes a nonsingular bounce. At the minisuperspace level, the Hamiltonian constraint constructed from that equation determines whether the Wheeler–DeWitt wave function is suppressed, regular, or oscillatory in the corresponding region. The second step is a quantization of the effective cosmological model; it does not derive the potential-inspired $\hbar$ term independently.

3. Minisuperspace Quantization and the Wheeler–DeWitt Equation

The Wheeler–DeWitt framework and its minisuperspace realization have a long history in quantum cosmology [3,14,35]. In this section, we quantize the scale-factor degree of freedom and derive a Wheeler–DeWitt-type equation associated with the modified Friedmann dynamics obtained in Section 2. We quantize an effective one-dimensional minisuperspace model whose Hamiltonian constraint is chosen so that its classical limit reproduces the modified Friedmann equation derived above. This construction is used as an effective quantum-cosmological model and is not intended as a fundamental or ultraviolet-complete quantization of the full gravitational field. This is sufficient for the present purpose, which is to determine how the running gravitational coupling modifies the quantum behavior of the scale factor.

The scale factor $a(t)$ is taken to be dimensionless, with the physical radius written as $R(t) = a(t)R_0$, where R_0 is a fixed reference length. Because a is dimensionless, the reduced minisuperspace action must retain the corresponding fiducial volume factor R_0^3. This factor ensures that the reduced Lagrangian has dimensions of energy and that the canonical momentum conjugate to a has dimensions of action. The constants c, $\hbar$, G_0, and R_0 are therefore kept explicitly throughout the derivation. Dimensionless units are introduced only after the equations have been written in a dimensionally consistent form.

3.1. Reduced Minisuperspace Dynamics

We begin with the effective gravitational kinetic term. Since the scale factor a is dimensionless, the fiducial spatial-volume factor R_0^3 must be retained. The kinetic term of the Lagrangian can be written as

$$L_{\rm kin}(a,\dot{a}) = -\frac{3\pi c^2 R_0^3}{4G(a)}\, a\dot{a}^{\,2}. \tag{63}$$

The reduced Lagrangian is then

$$L(a,\dot{a}) = L_{\rm kin}(a,\dot{a}) - V(a), \tag{64}$$

where $V(a)$ denotes the effective minisuperspace potential. In the present model, $V(a)$ contains the matter contribution, the curvature term, the higher-order classical correction, and the quantum correction.

The canonical momentum conjugate to a is

$$p_a \equiv \frac{\partial L}{\partial \dot{a}} = -\frac{3\pi c^2 R_0^3}{2G(a)}\, a\dot{a}, \tag{65}$$

so that

$$\dot{a} = -\frac{2G(a)}{3\pi c^2 R_0^3}\frac{p_a}{a}. \tag{66}$$

The corresponding Hamiltonian is

$$\mathcal{H} = p_a\dot{a} - L = -\frac{G(a)}{3\pi c^2 R_0^3 a}p_a^2 + V(a). \tag{67}$$

The classical dynamics are obtained from the Hamiltonian constraint

$$\mathcal{H} = 0. \tag{68}$$

Using Equation (65), the constraint implies

$$H^2(a) \equiv \left(\frac{\dot{a}}{a}\right)^2 = \frac{4G(a)}{3\pi c^2 R_0^3}\frac{V(a)}{a^3}. \tag{69}$$

Rearranging,

$$V(a) = \frac{3\pi c^2 R_0^3}{4G(a)} a^3 H^2(a). \tag{70}$$

Thus, the effective potential is not introduced independently; it is fixed by the modified Friedmann function $H^2(a)$.

For the scale-dependent gravity model considered here,

$$\begin{aligned} H^2(a) =& \frac{8\pi}{3} G^*(a)\rho_0 a^{-3\gamma} + \Upsilon_{\rm cl}\frac{32\pi^2}{9c^2} G_1^{*2}(a)\rho_0^2 a^{2-6\gamma} \\ & - \Xi\frac{8\pi}{3}\frac{\hbar}{c^3} G_2^{*2}(a)\rho_0 a^{-(3\gamma+2)} - \frac{kc^2}{a^2}. \end{aligned} \tag{71}$$

This is the same modified Friedmann equation derived in Section 2. The dimensional normalization of the reduced minisuperspace action does not alter the classical function $H^2(a)$; instead, it determines the dimensionally consistent coefficient with which $H^2(a)$ enters the effective Wheeler–DeWitt potential.

3.2. Factor Ordering and Wheeler–DeWitt Equation

Upon quantization, we promote

$$p_a \to -i\hbar\frac{d}{da}. \tag{72}$$

Since a is dimensionless and the corrected momentum (65) has dimensions of action, the two sides of Equation (72) have the same dimensions.

Because the scale factor is a minisuperspace variable, the ordering of p_a^2 is not unique. We adopt the standard one-parameter factor-ordering prescription

$$p_a^2\psi(a) \longrightarrow -\hbar^2\left(\frac{d^2\psi}{da^2} + \frac{q}{a}\frac{d\psi}{da}\right), \tag{73}$$

where q is the factor-ordering parameter. This convention includes commonly used choices in minisuperspace quantum cosmology, while making explicit that different orderings can shift the subleading behavior of the wave function near $a = 0$ [3,14,35]. The parameter q represents the factor-ordering ambiguity of the reduced minisuperspace model. We retain it explicitly and examine representative choices below; no unique ordering prescription is assumed.

The Wheeler–DeWitt equation $\widehat{\mathcal{H}}\psi = 0$ is therefore

$$\frac{\hbar^2 G(a)}{3\pi c^2 R_0^3 a}\left[\frac{d^2\psi}{da^2} + \frac{q}{a}\frac{d\psi}{da}\right] + V(a)\psi(a) = 0. \tag{74}$$

Eliminating $V(a)$ with Equation (70), we obtain the compact form

$$\frac{d^2\psi}{da^2} + \frac{q}{a}\frac{d\psi}{da} + \frac{9\pi^2 c^4 R_0^6}{4\hbar^2 G(a)^2} a^4 H^2(a)\psi(a) = 0. \tag{75}$$

This equation is the central quantum equation used in the remainder of the paper. It shows explicitly how the running gravitational coupling enters the Wheeler–DeWitt potential through both $G(a)$ and the modified Friedmann function $H^2(a)$.

3.3. Power-Law Running

We now specialize to the power-law running

$$G(a) = G_0 a^n. \tag{76}$$

Using the starred couplings derived in Section 2,

$$G^*(a) = \frac{G_0}{1-n} a^n, \qquad G_1^{*2}(a) = \frac{G_0^2}{1-n} a^{2n}, \qquad G_2^{*2}(a) = -\frac{3G_0^2}{2n-3} a^{2n}, \tag{77}$$

valid for $n \neq 1$ and $n \neq 3/2$, Equation (75) becomes

$$\psi''(a) + \frac{q}{a}\psi'(a) + \frac{9\pi^2 c^4 R_0^6}{4\hbar^2 G_0^2} a^{4-2n} H^2(a)\psi(a) = 0. \tag{78}$$

The corresponding Friedmann function is

$$\begin{aligned} H^2(a) =& \frac{8\pi}{3}\frac{G_0}{1-n}\rho_0 a^{n-3\gamma} + \Upsilon_{\rm cl}\frac{32\pi^2}{9c^2}\frac{G_0^2}{1-n}\rho_0^2 a^{2n+2-6\gamma} \\ &+ \Xi\frac{8\pi\hbar}{c^3}\frac{G_0^2}{2n-3}\rho_0 a^{2n-(3\gamma+2)} - \frac{kc^2}{a^2}. \end{aligned} \tag{79}$$

Substitution gives the expanded Wheeler–DeWitt equation

$$\begin{aligned} \psi''(a) + \frac{q}{a}\psi'(a) + \Bigg[& \frac{6\pi^3 c^4 R_0^6 \rho_0}{\hbar^2(1-n)G_0} a^{4-n-3\gamma} \\ & + \Upsilon_{\rm cl}\frac{8\pi^4 c^2 R_0^6 \rho_0^2}{\hbar^2(1-n)} a^{6-6\gamma} \\ & + \Xi\frac{18\pi^3 c R_0^6 \rho_0}{\hbar(2n-3)} a^{2-3\gamma} \\ & - \frac{9\pi^2 k c^6 R_0^6}{4\hbar^2 G_0^2} a^{2-2n} \Bigg] \psi(a) = 0. \end{aligned} \tag{80}$$

The running exponent n changes the powers of a appearing in the Wheeler–DeWitt potential. Thus, the small-scale behavior of the wave function is controlled by the matter equation of state, the factor ordering, and the scaling behavior of the gravitational coupling itself.

3.4. Representative Analytic and Numerical Solutions

We now examine representative solutions of Equation (80) where we wish to display the main types of behavior admitted by the model. We focus on flat models with

$$k = 0, \qquad \Upsilon_{\rm cl} = 0,$$

so that the competition between the ordinary matter term and the Ξ-induced quantum correction can be highlighted. Exact and semiclassical solutions of the Wheeler–DeWitt equation are known in special minisuperspace settings [15,35], and the present model provides additional tractable examples in which the effect of the running gravitational coupling can be seen explicitly.

For $n = 2$, the ordinary matter contribution and the Ξ-dependent quantum correction in Equation (80) scale with the same power of a. The Wheeler–DeWitt equation then reduces to

$$\psi''(a) + \frac{q}{a}\psi'(a) + \lambda_{\rm eff} a^{2-3\gamma}\psi(a) = 0, \tag{81}$$

where

$$\lambda_{\rm eff} = -\frac{6\pi^3 c^4 R_0^6 \rho_0}{\hbar^2 G_0} + \frac{18\pi^3 \Xi c R_0^6 \rho_0}{\hbar}. \tag{82}$$

For the representative choice

$$\Xi = \frac{\xi_{\rm QG}}{R_0^2}, \qquad \xi_{\rm QG} = \frac{122}{15\pi}, \tag{83}$$

this becomes

$$\lambda_{\rm eff} = -\frac{6\pi^3 c^4 R_0^6 \rho_0}{\hbar^2 G_0} + \frac{732}{5}\pi^2 \frac{c R_0^4 \rho_0}{\hbar}. \tag{84}$$

In the examples below, we take $\lambda_{\rm eff} > 0$, so that the solutions are oscillatory at a sufficiently large scale factor. If $\lambda_{\rm eff} < 0$, the corresponding solutions are expressed in terms of modified Bessel functions, and the oscillatory interpretation must be modified.

3.4.1. Dust-Era Bessel Solution Satisfying the DeWitt Condition

For a dust-dominated universe, $\gamma = 1$, Equation (81) becomes

$$\psi''(a) + \frac{q}{a}\psi'(a) + \lambda_{\rm eff} a^{-1}\psi(a) = 0. \tag{85}$$

The general solution is

$$\psi(a) = a^{(1-q)/2}\left[C_1 J_{1-q}\left(2\sqrt{\lambda_{\rm eff} a}\right) + C_2 Y_{1-q}\left(2\sqrt{\lambda_{\rm eff} a}\right)\right]. \tag{86}$$

The Y_{1-q} branch is singular at the origin and is discarded if regularity at $a = 0$ is required. The regular branch is therefore

$$\psi(a) = C\, a^{(1-q)/2} J_{1-q}\left(2\sqrt{\lambda_{\rm eff} a}\right). \tag{87}$$

Near the origin,

$$\psi(a) \sim a^{1-q}. \tag{88}$$

Thus, this branch satisfies the DeWitt boundary condition,

$$\psi(0) = 0, \tag{89}$$

whenever $q < 1$. The DeWitt condition is commonly interpreted as suppression of the classical singular geometry in the quantum theory [3].

At large a, the Bessel asymptotics give

$$\psi(a) \sim a^{(1-2q)/4} \cos\left[2\sqrt{\lambda_{\rm eff} a} - \frac{\pi}{2}(1-q) - \frac{\pi}{4}\right]. \tag{90}$$

The envelope decays for $1/2 < q < 1$, is asymptotically constant for $q = 1/2$, and grows for $q < 1/2$.

An illustrative parameterization is

$$q = \frac{3}{4}, \tag{91}$$

for which

$$\psi(a) = C\, a^{1/8} J_{1/4}\left(2\sqrt{\lambda_{\rm eff} a}\right). \tag{92}$$

This solution vanishes at $a = 0$, satisfies the DeWitt criterion, and exhibits damped oscillations at a large scale factor (see Figure 2). It therefore provides a simple analytic example of a state that is suppressed near the classical singularity and becomes semiclassical in the large-a regime.

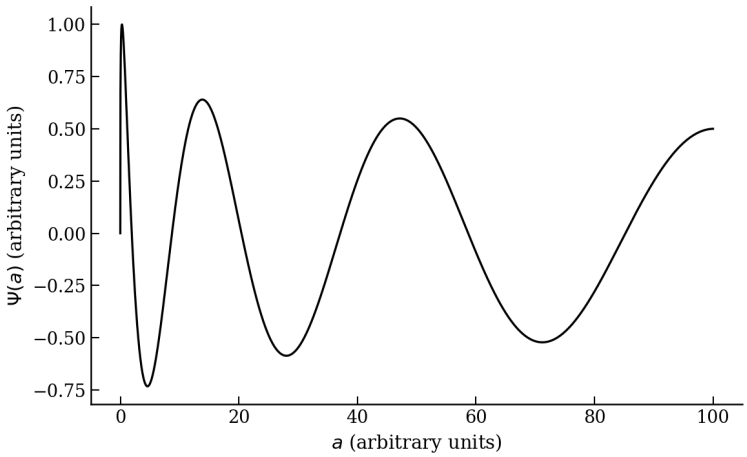


Figure 2. Dust-case Wheeler–DeWitt wave function for $n = 2$, $\gamma = 1$, $q = \frac{3}{4}$, $k = \mathrm{Y_{cl}} = 0$, with $\xi_{\rm QG} = 122/(15\pi)$ and $\Xi = \xi_{\rm QG}/R_0^2$. The exact solution $\psi(a) \propto a^{1/8} J_{1/4}(2\sqrt{\lambda_{\rm eff} a})$ vanishes at $a = 0$, satisfying the DeWitt boundary condition, and exhibits damped oscillations for increasing scale factor.

3.4.2. Regular Dust-Era Solution Without DeWitt Suppression

The case $q = 1$ results in a useful comparison. Equation (86) becomes

$$\psi(a) = C_1 J_0\left(2\sqrt{\lambda_{\rm eff} a}\right) + C_2 Y_0\left(2\sqrt{\lambda_{\rm eff} a}\right). \tag{93}$$

Since $Y_0(x)$ diverges logarithmically as $x \to 0$, regularity at the origin selects

$$\psi(a) = C\, J_0\left(2\sqrt{\lambda_{\rm eff} a}\right). \tag{94}$$

However,

$$J_0(0) = 1, \tag{95}$$

so this solution (see Figure 3) is finite but nonzero at $a = 0$. It therefore satisfies a regularity condition, but not the stronger DeWitt condition. A regular nonzero wave function at the origin is more naturally interpreted as a regular quantum origin than as strict DeWitt suppression of the singular geometry. This is closer in spirit to the Hartle–Hawking regularity viewpoint than to imposing $\psi(0) = 0$ as a boundary condition [4].

For large a,

$$\psi(a) \sim a^{-1/4} \cos\left(2\sqrt{\lambda_{\rm eff} a} - \frac{\pi}{4}\right), \tag{96}$$

so the solution is again oscillatory with a slowly decaying envelope. The factor-ordering parameter therefore controls whether the origin is regular or suppressed.

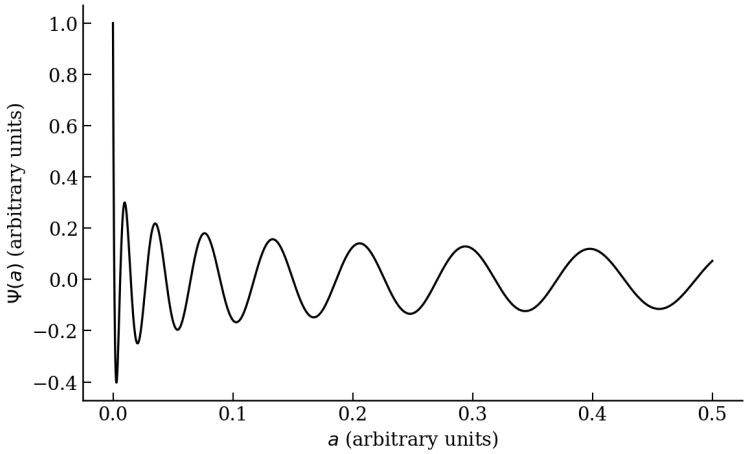


Figure 3. Dust-case Wheeler–DeWitt wave function for $n = 2$, $\gamma = 1$, $q = 1$, $k = \mathrm{Y_{cl}} = 0$, with $\xi_{\mathrm{QG}} = 122/(15\pi)$ and $\Xi = \xi_{\mathrm{QG}}/R_0^2$. The regular solution $\psi(a) \propto J_0(2\sqrt{\lambda_{\mathrm{eff}} a})$ remains finite and nonzero at $a = 0$. It therefore satisfies regularity at the origin, but not the DeWitt boundary condition.

3.4.3. A Non-Bessel Airy Example

The model also admits exact analytic sectors that are not of Bessel type. For

$$n = 2, \qquad \gamma = \frac{1}{3}, \qquad q = 0, \qquad k = \mathrm{Y_{cl}} = 0,$$

Equation (81) becomes

$$\psi''(a) + \lambda_{\mathrm{eff}} a\, \psi(a) = 0. \tag{97}$$

Defining

$$x = -\lambda_{\mathrm{eff}}^{1/3} a, \tag{98}$$

this becomes the standard Airy equation,

$$\frac{d^2\psi}{dx^2} - x\psi = 0. \tag{99}$$

The general solution is

$$\psi(a) = C_1 \mathrm{Ai}\left(-\lambda_{\mathrm{eff}}^{1/3} a\right) + C_2 \mathrm{Bi}\left(-\lambda_{\mathrm{eff}}^{1/3} a\right). \tag{100}$$

A DeWitt-compatible linear combination is obtained by imposing $\psi(0) = 0$. Since

$$\frac{\mathrm{Ai}(0)}{\mathrm{Bi}(0)} = \frac{1}{\sqrt{3}}, \tag{101}$$

one obtains

$$\psi(a) = C\left[\mathrm{Ai}\left(-\lambda_{\mathrm{eff}}^{1/3} a\right) - \frac{1}{\sqrt{3}} \mathrm{Bi}\left(-\lambda_{\mathrm{eff}}^{1/3} a\right)\right]. \tag{102}$$

This solution (see Figure 4) vanishes at $a = 0$ by construction and becomes oscillatory for large positive a. Although $\gamma = 1/3$ corresponds to an exotic equation of state rather than ordinary dust or radiation, the example is revealing because it shows that the scale-dependent model supports exact non-Bessel wave-function sectors.

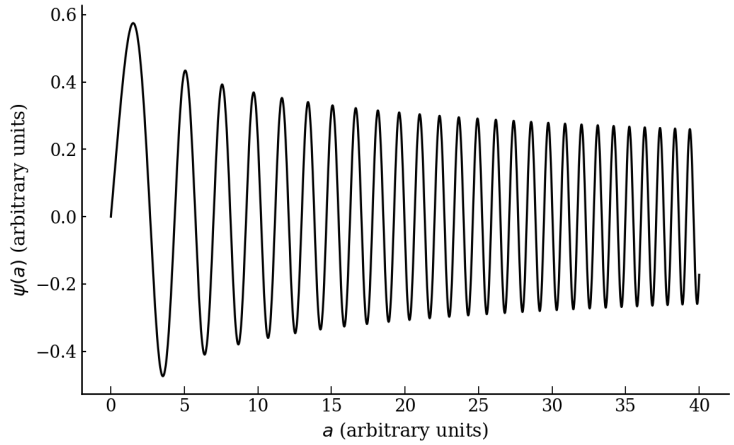


Figure 4. Airy-type Wheeler–DeWitt wave function for $n = 2$, $\gamma = \frac{1}{3}$, $q = 0$, $k = \mathrm{Y_{cl}} = 0$, with $\xi_{\mathrm{QG}} = 122/(15\pi)$ and $\Xi = \xi_{\mathrm{QG}}/R_0^2$. The linear combination $\psi(a) \propto \mathrm{Ai}(-\lambda_{\mathrm{eff}}^{1/3} a) - \mathrm{Bi}(-\lambda_{\mathrm{eff}}^{1/3} a)/\sqrt{3}$ is chosen so that $\psi(0) = 0$, thereby satisfying the DeWitt condition.

3.4.4. Numerical Radiation-Era Example

As a radiation-era example, consider a radiation-dominated universe with

$$\gamma = \frac{4}{3}, \qquad n = -1, \qquad q = 0, \qquad k = \mathrm{Y_{cl}} = 0, \qquad \xi_{\mathrm{QG}} = \frac{122}{15\pi}, \qquad \Xi = \frac{\xi_{\mathrm{QG}}}{R_0^2}. \tag{103}$$

In this case, Equation (80) has the schematic form

$$\psi''(a) + \left(Aa - \frac{B}{a^2}\right)\psi(a) = 0, \qquad A > 0, \quad B > 0, \tag{104}$$

after collecting constants. The inverse-square term dominates as $a \to 0$ and produces a suppressed regular branch. At larger scale factors the positive linear term dominates, leading to an oscillatory regime. The numerical solution (see Figure 5) therefore transitions from suppression near $a = 0$ to oscillatory behavior at larger a.

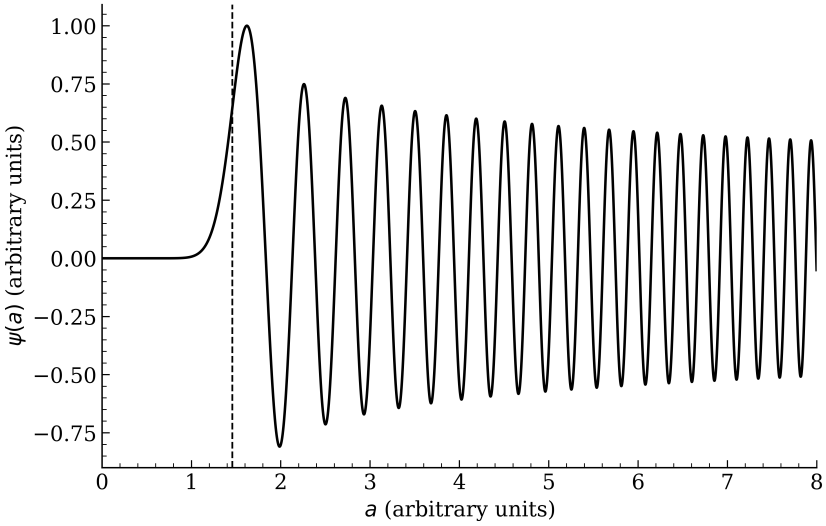


Figure 5. Numerical Wheeler–DeWitt wave function for the radiation-dominated case $\gamma = \frac{4}{3}$, with $n = -1$, $q = 0$, $k = 0$, $\mathrm{Y_{cl}} = 0$, using $\xi_{\mathrm{QG}} = 122/(15\pi)$ and $\Xi = \xi_{\mathrm{QG}}/R_0^2$. The regular branch is suppressed near $a = 0$, satisfying the DeWitt condition, and becomes oscillatory at larger scale factors. The dashed vertical line marks the zero of the effective coefficient in Equation (104), separating the suppressed small-a region from the oscillatory large-a region.

3.5. Local Airy Form near a Turning Point

Before turning to the full WKB analysis, we examine the local behavior near a simple turning point. Removing the first-derivative term by writing

$$\psi(a) = a^{-q/2}u(a), \tag{105}$$

the Wheeler–DeWitt equation takes the reduced form

$$u''(a) + U_{\text{eff}}(a)u(a) = 0. \tag{106}$$

Suppose that the effective potential has a simple turning point $a = a_t$, so that

$$U_{\text{eff}}(a_t) = 0, \qquad U'_{\text{eff}}(a_t) \neq 0. \tag{107}$$

Expanding linearly,

$$U_{\text{eff}}(a) \simeq U'_{\text{eff}}(a_t)(a - a_t), \tag{108}$$

Equation (106) reduces to Airy's equation. The local solution may be written as

$$u(a) = c_1 \text{Ai}\left(\frac{a_t - a}{s}\right) + c_2 \text{Bi}\left(\frac{a_t - a}{s}\right), \qquad s = \left[U'_{\text{eff}}(a_t)\right]^{-1/3}, \tag{109}$$

up to the sign convention associated with $U'_{\text{eff}}(a_t)$. Selecting the Ai branch gives exponential suppression on the forbidden side of the turning point and oscillatory behavior on the allowed side (see Figure 6). This is the standard local structure underlying WKB matching in quantum cosmology [4,5].

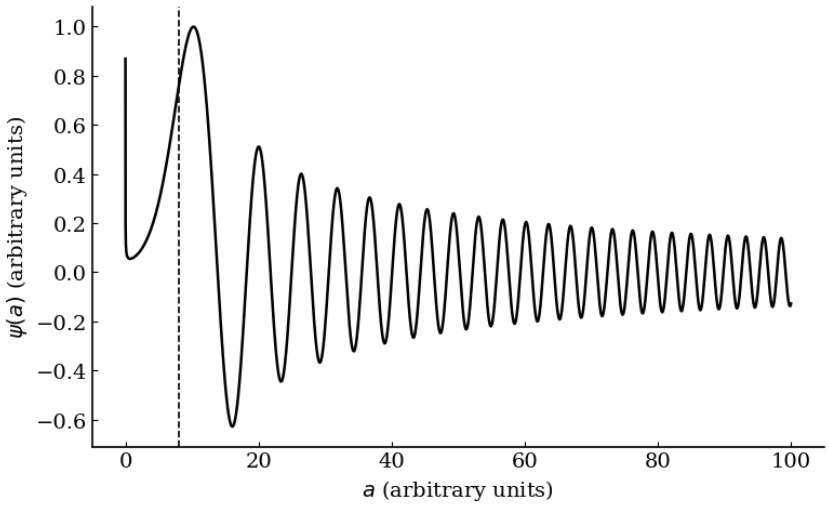


Figure 6. Illustrative Airy-type semiclassical Wheeler–DeWitt wave function near a single turning point a_t. The local form $\psi(a) = a^{-q/2}\text{Ai}((a_t - a)/s)$, shown here for $q = 1$, is exponentially suppressed on the forbidden side of the turning point and oscillatory on the allowed side. This figure illustrates the universal Airy matching behavior that appears near a simple Wheeler–DeWitt turning point. The vertical dashed line indicates the turning point.

3.6. Summary of the Wheeler–DeWitt Sectors

The examples above show that the scale-dependent model admits several distinct quantum behaviors. The dust solution with $q = \frac{3}{4}$ is revealing: it is analytic, physically transparent, satisfies the DeWitt condition, and has a damped oscillatory large-a limit. The $q = 1$ dust solution shows that regularity at $a = 0$ is not the same as DeWitt suppression. The Airy example illustrates that the model is not restricted to Bessel-type sectors, while

the radiation-era numerical solution provides a more familiar matter source in which the small-a region is suppressed and the large-a regime becomes oscillatory.

These results prepare us for the WKB analysis in Section 4. There, the same effective potential structure will be used to identify forbidden and allowed regions, turning points, and the branch interpretation of the minisuperspace wave function.

4. WKB Dynamics, Turning Points, and Probability Current

The exact solutions discussed in Section 3 show explicitly that the scale-dependent model admits wave functions that are either suppressed at the classical singularity or regular at the origin. We now turn to the WKB regime, where the connection between the Wheeler–DeWitt wave function and classical cosmological dynamics becomes explicit. The purpose of this section is to show how a forbidden small-a region, a turning point, and an oscillatory large-a branch arise in a representative case, and how the probability current distinguishes expanding and contracting semiclassical sectors.

We consider the flat dust-dominated model

$$\gamma = 1, \qquad n = 3, \qquad q = 1, \qquad k = 0, \qquad \Upsilon_{\rm cl} = 0, \tag{110}$$

with the one-loop quantum-correction coefficient specified by

$$\xi_{\rm QG} = \frac{122}{15\pi}, \qquad \Xi = \frac{\xi_{\rm QG}}{R_0^2}. \tag{111}$$

This example is instructive because it reduces the Wheeler–DeWitt equation to a single-turning-point problem while retaining the effect of the running gravitational coupling. The resulting WKB structure is the familiar one: exponential behavior in a forbidden region, Airy matching near the turning point, and oscillatory behavior in the allowed region [4,5,36].

4.1. Reduced Wheeler–DeWitt Equation for a Chosen Model

We begin with the power-law Wheeler–DeWitt equation derived in Section 3,

$$\psi''(a) + \frac{q}{a}\psi'(a) + \frac{9\pi^2 c^4 R_0^6}{4\hbar^2 G_0^2} a^{4-2n} H^2(a)\psi(a) = 0. \tag{112}$$

For $q = 1$ and $n = 3$, this becomes

$$\psi''(a) + \frac{1}{a}\psi'(a) + \frac{9\pi^2 c^4 R_0^6}{4\hbar^2 G_0^2} a^{-2} H^2(a)\psi(a) = 0. \tag{113}$$

For dust matter, $\gamma = 1$, with $k = 0$ and $\Upsilon_{\rm cl} = 0$, the modified Friedmann function reduces to

$$H^2(a) = \frac{8\pi}{3}\frac{G_0}{1-3}\rho_0 a^{3-3} + \Xi\frac{8\pi\hbar}{c^3}\frac{G_0^2}{2\cdot 3-3}\rho_0 a^{6-(3+2)}. \tag{114}$$

Hence,

$$H^2(a) = -\frac{4\pi}{3} G_0\rho_0 + \Xi\frac{8\pi\hbar}{3c^3} G_0^2\rho_0\, a. \tag{115}$$

Using

$$\Xi = \frac{\xi_{\rm QG}}{R_0^2}, \qquad \xi_{\rm QG} = \frac{122}{15\pi},$$

Equation (115) becomes

$$H^2(a) = -\frac{4\pi}{3} G_0 \rho_0 + \frac{976}{45} \frac{\hbar G_0^2 \rho_0}{c^3 R_0^2}\, a. \tag{116}$$

Substituting Equation (115) into Equation (113) gives

$$\psi''(a) + \frac{1}{a}\psi'(a) + \left(\frac{\beta}{a} - \frac{\mu}{a^2}\right)\psi(a) = 0, \tag{117}$$

where

$$\mu = \frac{3\pi^3 c^4 R_0^6 \rho_0}{\hbar^2 G_0}, \qquad \beta = \frac{6\pi^3 \Xi c R_0^6 \rho_0}{\hbar}. \tag{118}$$

Using

$$\Xi = \frac{\xi_{\mathrm{QG}}}{R_0^2}, \qquad \xi_{\mathrm{QG}} = \frac{122}{15\pi},$$

the coefficient becomes

$$\beta = \frac{6\pi^3 \xi_{\mathrm{QG}} c R_0^4 \rho_0}{\hbar} = \frac{244}{5}\pi^2 \frac{c R_0^4 \rho_0}{\hbar}. \tag{119}$$

To remove the first-derivative term, we define

$$\psi(a) = a^{-1/2}\phi(a). \tag{120}$$

Then, Equation (117) becomes

$$\phi''(a) + Q(a)\phi(a) = 0, \tag{121}$$

with

$$Q(a) = \frac{\beta}{a} - \frac{\alpha}{a^2}, \qquad \alpha = \mu - \frac{1}{4} = \frac{3\pi^3 c^4 R_0^6 \rho_0}{\hbar^2 G_0} - \frac{1}{4}. \tag{122}$$

Equivalently,

$$Q(a) = \frac{\beta a - \alpha}{a^2}. \tag{123}$$

4.2. Turning Point and WKB Regions

The turning point is determined by

$$Q(a_t) = 0. \tag{124}$$

For $\alpha > 0$ and $\beta > 0$, this gives the single positive turning point

$$a_t = \frac{\alpha}{\beta}. \tag{125}$$

The sign of $Q(a)$ then separates minisuperspace into two regions:

$$Q(a) < 0, \qquad 0 < a < a_t, \tag{126}$$

and

$$Q(a) > 0, \qquad a > a_t. \tag{127}$$

Thus, the small-a region is WKB-forbidden, while the large-a region is WKB-allowed. This yields a forbidden small-a region and an allowed oscillatory large-a region.

For the dimensionless illustration below, we scale all quantities by fixed reference values and denote the resulting dimensionless coefficients by $\widehat{\alpha}$ and $\widehat{\beta}$. The numerical example is chosen so that

$$\widehat{\alpha} \simeq 92.769, \qquad \widehat{\beta} \simeq 481.637, \qquad a_t = \frac{\widehat{\alpha}}{\widehat{\beta}} \simeq 0.193. \tag{128}$$

These values specify an illustrative dimensionless model and should not be interpreted as a direct substitution of measured cosmological quantities in Planck units.

4.3. Forbidden-Region and Allowed-Region Solutions

In the forbidden region $0 < a < a_t$, define

$$\kappa(a) = \sqrt{|Q(a)|} = \frac{\sqrt{\alpha - \beta a}}{a}. \tag{129}$$

The WKB solution for $\phi(a)$ is

$$\phi_{\text{forb}}(a) \approx |Q(a)|^{-1/4}\Big[Ae^{-I(a)} + Be^{+I(a)}\Big], \tag{130}$$

where

$$I(a) = \int_a^{a_t} \kappa(a')\, da'. \tag{131}$$

Since $\psi(a) = a^{-1/2}\phi(a)$, the corresponding WKB form for the original wave function is

$$\psi_{\text{forb}}(a) \approx (\alpha - \beta a)^{-1/4}\Big[Ae^{-I(a)} + Be^{+I(a)}\Big]. \tag{132}$$

The branch proportional to $e^{-I(a)}$ is suppressed as $a \to 0$. Selecting this branch gives a wave function that is exponentially small in the classically forbidden small-a region.

In the allowed region $a > a_t$, define

$$p(a) = \sqrt{Q(a)} = \frac{\sqrt{\beta a - \alpha}}{a}. \tag{133}$$

The WKB solution for $\phi(a)$ is

$$\phi_{\text{all}}(a) \approx Q(a)^{-1/4}\Big[Ce^{i\Theta(a)} + De^{-i\Theta(a)}\Big], \tag{134}$$

where

$$\Theta(a) = \int_{a_t}^{a} p(a')\, da'. \tag{135}$$

Thus, the original wave function is

$$\psi_{\text{all}}(a) \approx (\beta a - \alpha)^{-1/4}\Big[Ce^{i\Theta(a)} + De^{-i\Theta(a)}\Big]. \tag{136}$$

4.4. Airy Matching near the Turning Point

The connection between the forbidden and allowed WKB regions is obtained by matching to the local Airy solution near $a = a_t$. Expanding $Q(a)$ about the turning point gives

$$Q(a) \simeq Q'(a_t)(a - a_t), \tag{137}$$

where, using $Q(a) = \beta/a - \alpha/a^2$,

$$Q'(a_t) = \frac{\beta^3}{\alpha^2} > 0. \tag{138}$$

Defining the local Airy scale

$$s = \left[Q'(a_t)\right]^{-1/3} = \left(\frac{\alpha^2}{\beta^3}\right)^{1/3}, \tag{139}$$

the reduced equation takes the standard Airy form near the turning point. The usual connection formula (see, e.g., [36,37]) gives the real matched solution in the allowed region as

$$\psi_{\rm all}(a) \approx (\beta a - \alpha)^{-1/4} \cos\left(\Theta(a) - \frac{\pi}{4}\right).$$

The $-\pi/4$ phase shift is the standard result for matching a decaying exponential on the forbidden side to an oscillatory solution on the allowed side.

This standing-wave form is the standard WKB continuation of a real decaying solution in the forbidden region. A purely outgoing or purely incoming branch may instead be selected by imposing an additional boundary condition in the allowed region.

4.5. Closed-Form WKB Actions and Asymptotic Behavior

For this case, the WKB actions can be evaluated analytically. In the forbidden region,

$$I(a) = 2\sqrt{\alpha}\left[\operatorname{artanh}\sqrt{1-\frac{a}{a_t}} - \sqrt{1-\frac{a}{a_t}}\right]. \tag{140}$$

This expression vanishes at the turning point and diverges logarithmically as $a \to 0$. Consequently, the decaying branch in Equation (132) is strongly suppressed near the classical singularity. In fact,

$$\psi(a) \sim a^{\sqrt{\alpha}}, \qquad a \to 0, \tag{141}$$

up to an overall constant.

In the allowed region,

$$\Theta(a) = 2\sqrt{\alpha}\left[\sqrt{\frac{a}{a_t}-1} - \arctan\sqrt{\frac{a}{a_t}-1}\right]. \tag{142}$$

For large a,

$$Q(a) \sim \frac{\beta}{a}, \tag{143}$$

and the phase behaves as

$$\Theta(a) \sim 2\sqrt{\beta a} - \pi\sqrt{\alpha}, \qquad a \to \infty. \tag{144}$$

Therefore, the large-a wave function has the asymptotic form

$$\psi(a) \sim (\beta a)^{-1/4} \cos\left(2\sqrt{\beta a} - \pi\sqrt{\alpha} - \frac{\pi}{4}\right), \qquad a \to \infty. \tag{145}$$

The large-scale wave function is therefore oscillatory with a slowly decaying envelope (see Figure 7). This is the usual WKB signature of a semiclassical regime.

The result is a WKB realization of the usual tunneling-type structure: a suppressed small-a region, a turning point, and an oscillatory large-a semiclassical branch. In the present model, this structure is generated by the scale dependence of the gravitational coupling and the associated quantum-correction Ξ-dependent term.

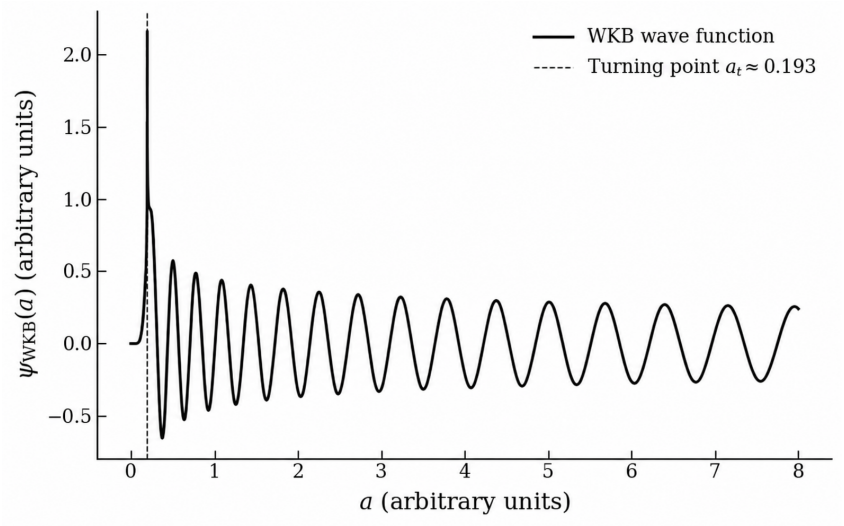


Figure 7. WKB wave function for the example case $\gamma = 1$, $n = 3$, $q = 1$, $\mathrm{Y_{cl}} = 0$, and $k = 0$, using the dimensionless coefficients $\widehat{\alpha}$ and $\widehat{\beta}$ specified in Equation (128). The dashed vertical line marks the turning point $a_t \simeq 0.193$, which separates the small-a WKB-forbidden region from the large-a WKB-allowed region. For $a < a_t$, the wave function is exponentially suppressed, while for $a > a_t$, it becomes oscillatory with a slowly decaying envelope.

4.6. Probability Current and Branch Interpretation

The WKB wave function becomes physically clearer when supplemented by the minisuperspace probability current. For the factor-ordered Wheeler–DeWitt equation

$$\psi''(a) + \frac{q}{a}\psi'(a) + \Omega(a)\psi(a) = 0, \tag{146}$$

with real $\Omega(a)$, the conserved current is

$$J_q(a) = \frac{1}{2i}a^q\left(\psi^*\psi' - \psi\psi^{*\prime}\right). \tag{147}$$

For the present model $q = 1$, this becomes

$$J(a) = \frac{1}{2i}a\left(\psi^*\psi' - \psi\psi^{*\prime}\right). \tag{148}$$

In the allowed region $a > a_t$, the outgoing and incoming WKB branches are

$$\psi_{\rm out}(a) \approx (\beta a - \alpha)^{-1/4}e^{i\Theta(a)}, \qquad \psi_{\rm in}(a) \approx (\beta a - \alpha)^{-1/4}e^{-i\Theta(a)}. \tag{149}$$

With the WKB branches normalized to unit minisuperspace flux, one obtains

$$J_{\rm out} = +1, \qquad J_{\rm in} = -1. \tag{150}$$

For an arbitrary overall wave-function normalization, the currents are multiplied by the corresponding squared amplitude. Thus, the outgoing branch carries positive flux, while the incoming branch carries negative flux. In this sense, the sign of the conserved current distinguishes expanding and contracting semiclassical branches [5].

By contrast, the real standing-wave combination

$$\psi_{\rm stand}(a) \approx 2(\beta a - \alpha)^{-1/4}\cos\left(\Theta(a) - \frac{\pi}{4}\right) \tag{151}$$

has

$$J_{\text{stand}} = 0. \tag{152}$$

Similarly, a purely real decaying solution in the forbidden region carries no current. A nonzero conserved flux therefore appears only after selecting a complex traveling-wave branch in the WKB-allowed region. This is why the current is an invaluable diagnostic: oscillatory behavior alone does not specify a direction of semiclassical evolution, while the current does.

For the illustrative choice of values in Equation (128), one finds numerically that the current is constant across the allowed region:

$$\langle J_{\text{out}} \rangle = 1, \qquad \langle J_{\text{in}} \rangle = -1, \qquad \langle J_{\text{stand}} \rangle = 0. \tag{153}$$

This confirms the branch interpretation of the WKB solutions.

4.7. Hamilton–Jacobi Limit and Classical Recovery

The WKB phase also explains how the classical modified Friedmann dynamics are recovered. Starting from the compact Wheeler–DeWitt equation,

$$\psi''(a) + \frac{q}{a}\psi'(a) + \frac{9\pi^2 c^4 R_0^6}{4\hbar^2 G(a)^2} a^4 H^2(a)\psi(a) = 0, \tag{154}$$

we use the WKB ansatz

$$\psi(a) = A(a)\exp\left(\frac{i}{\hbar}S(a)\right). \tag{155}$$

At leading order in the WKB expansion, the phase satisfies

$$\left(\frac{dS}{da}\right)^2 = \frac{9\pi^2 c^4 R_0^6}{4G(a)^2} a^4 H^2(a). \tag{156}$$

Identifying

$$p_a = \frac{dS}{da} \tag{157}$$

and using the minisuperspace momentum

$$p_a = -\frac{3\pi c^2 R_0^3}{2G(a)} a\dot{a}, \tag{158}$$

one immediately obtains

$$\left(\frac{dS}{da}\right)^2 = \frac{9\pi^2 c^4 R_0^6}{4G(a)^2} a^2 \dot{a}^2 = \frac{9\pi^2 c^4 R_0^6}{4G(a)^2} a^4 H^2(a). \tag{159}$$

Thus, the WKB Hamilton–Jacobi equation is exactly the classical modified Friedmann dynamics written in canonical form. The phase of the Wheeler–DeWitt wave function therefore encodes the classical cosmological trajectory [14,17].

The factor-ordering term affects the transport equation for the WKB amplitude, but not the leading Hamilton–Jacobi relation. The Ξ-dependent term should be interpreted separately from the minisuperspace quantization: it is inherited from the potential-inspired effective Friedmann-type equation constructed in Section 2. The WKB expansion is therefore a semiclassical expansion of an effective minisuperspace model containing an explicit $\hbar$-dependent phenomenological term. It does not provide an independent derivation of that term.

The physical picture is then consistent across the classical and quantum descriptions. The roots of $H^2(a)$ determine the classical turning points. The same roots enter the Wheeler–DeWitt potential and determine where the WKB wave function changes from exponential to oscillatory behavior. In the oscillatory regime, the probability current separates expanding and contracting branches. In this way, the WKB analysis connects the modified Friedmann dynamics, the minisuperspace wave function, and the emergence of semiclassical cosmological evolution.

5. Wheeler–DeWitt Equation with a Scalar-Field Clock

The Wheeler–DeWitt equation derived above is a constraint equation, so it does not contain an external time variable. To give the quantum theory a relational interpretation, we enlarge the minisuperspace from the single variable a to (a, ϕ), where ϕ is a homogeneous free scalar field. Since the scalar-field momentum is conserved, ϕ can be used as an internal clock on any classical branch for which $p_\phi \neq 0$ [17,38]. This restriction becomes explicit in the exact relational trajectory (Equation (181)) and in its test-field reduction (Equation (183)) below.

We begin with the gravitational kinetic term used in the minisuperspace construction,

$$L_{g,\mathrm{kin}} = -\frac{3\pi c^2 R_0^3}{4G(a)} \frac{a\dot{a}^2}{N}, \tag{160}$$

where the lapse function $N(t)$ has been restored. For a homogeneous free scalar field, $V(\phi) = 0$, the corresponding kinetic term is

$$L_{\phi,\mathrm{kin}} = \frac{\pi^2 R_0^3 a^3}{N} \dot{\phi}^2. \tag{161}$$

The canonical momenta are therefore

$$p_a = -\frac{3\pi c^2 R_0^3}{2G(a)} \frac{a\dot{a}}{N}, \qquad p_\phi = \frac{2\pi^2 R_0^3 a^3}{N} \dot{\phi}. \tag{162}$$

Solving for the velocities and performing the Legendre transform gives the kinetic part of the Hamiltonian constraint,

$$\mathcal{H}_{\mathrm{kin}} = -\frac{G(a)}{3\pi c^2 R_0^3 a} p_a^2 + \frac{1}{4\pi^2 R_0^3 a^3} p_\phi^2. \tag{163}$$

The modified Friedmann equation can be written in the compact form

$$H^2(a) = F(a), \qquad H = \frac{\dot{a}}{a}, \tag{164}$$

where $F(a)$ denotes the full right-hand side of the scale-dependent modified Friedmann equation. The Hamiltonian constraint consistent with this classical limit is

$$\mathcal{H} = -\frac{G(a)}{3\pi c^2 R_0^3 a} p_a^2 + \frac{1}{4\pi^2 R_0^3 a^3} p_\phi^2 + \frac{3\pi c^2 R_0^3}{4G(a)} a^3 F(a) = 0. \tag{165}$$

Hence, if $p_\phi = 0$ and $N = 1$, then $p_a = -((3\pi c^2 R_0^3)/2G) a\dot{a}$, and Equation (165) reduces to $\dot{a}^2 = a^2 F(a)$, as required.

Upon quantization, we take

$$p_a \to -i\hbar \partial_a, \qquad p_\phi \to -i\hbar \partial_\phi, \tag{166}$$

and use the same factor ordering as above,

$$p_a^2 \to -\hbar^2\left(\partial_a^2 + \frac{q}{a}\partial_a\right). \tag{167}$$

The Wheeler–DeWitt equation in the two-dimensional minisuperspace is then

$$\left[\frac{G(a)\hbar^2}{3\pi c^2 R_0^3 a}\left(\partial_a^2 + \frac{q}{a}\partial_a\right) - \frac{\hbar^2}{4\pi^2 R_0^3 a^3}\partial_\phi^2 + \frac{3\pi c^2 R_0^3}{4G(a)}a^3 F(a)\right]\Psi(a,\phi) = 0. \tag{168}$$

Multiplying by $3\pi c^2 R_0^3 a/[G(a)\hbar^2]$, we obtain the more convenient form

$$\left[\partial_a^2 + \frac{q}{a}\partial_a - \frac{3c^2}{4\pi G(a)a^2}\partial_\phi^2 + \frac{9\pi^2 c^4 R_0^6}{4\hbar^2 G(a)^2}a^4 F(a)\right]\Psi(a,\phi) = 0. \tag{169}$$

This equation shows the structural change caused by the scalar clock: the scalar-field kinetic term enters with a coefficient proportional to $[G(a)a^2]^{-1}$. Thus, the same running gravitational coupling that modifies $F(a)$ also modifies the clock term itself.

For the power-law model

$$G(a) = G_0 a^n, \tag{170}$$

the scalar-clock contribution scales as

$$-\frac{3c^2}{4\pi G(a)a^2}\partial_\phi^2 = -\frac{3c^2}{4\pi G_0}a^{-(n+2)}\partial_\phi^2. \tag{171}$$

Hence, the standard inverse-square clock term is recovered only when $n = 0$. For $n > 0$, the scalar-clock term becomes more singular as $a \to 0$, while for $n < 0$, it is softened.

We now separate variables by writing

$$\Psi(a,\phi) = e^{i\omega\phi}\chi_\omega(a), \tag{172}$$

where ω is the conserved scalar-field frequency. Since $\partial_\phi^2\Psi = -\omega^2\Psi$, Equation (169) becomes

$$\chi_\omega''(a) + \frac{q}{a}\chi_\omega'(a) + \left[\frac{3c^2\omega^2}{4\pi G(a)a^2} + \frac{9\pi^2 c^4 R_0^6}{4\hbar^2 G(a)^2}a^4 F(a)\right]\chi_\omega(a) = 0. \tag{173}$$

For $G(a) = G_0 a^n$, this is

$$\chi_\omega''(a) + \frac{q}{a}\chi_\omega'(a) + \left[\frac{3c^2\omega^2}{4\pi G_0}a^{-(n+2)} + \frac{9\pi^2 c^4 R_0^6}{4\hbar^2 G_0^2}a^{4-2n}F(a)\right]\chi_\omega(a) = 0. \tag{174}$$

Using the normalized-density Friedmann function,

$$F(a) = \left(\frac{\Omega_0 H_0^2}{G_0}\right)G^*(a)a^{-3\gamma} + \Upsilon_{\rm cl}\left(\frac{\Omega_0^2 H_0^4}{2G_0^2 c^2}\right)G_1^{*2}(a)a^{2-6\gamma} - \Xi\left(\frac{\Omega_0 H_0^2}{G_0}\right)\frac{\hbar}{c^3}G_2^{*2}(a)a^{-(3\gamma+2)} - \frac{kc^2}{a^2},$$

and the power-law effective couplings

$$G^*(a) = \frac{G_0}{1-n}a^n, \qquad G_1^{*2}(a) = \frac{G_0^2}{1-n}a^{2n}, \qquad G_2^{*2}(a) = -\frac{3G_0^2}{2n-3}a^{2n}, \tag{175}$$

with $n \neq 1$ and $n \neq 3/2$, Equation (174) may be written as

$$\chi_\omega''(a) + \frac{q}{a}\chi_\omega'(a) + \left[\frac{3c^2\omega^2}{4\pi G_0}a^{-(n+2)} + Aa^{4-n-3\gamma} + Ba^{6-6\gamma} + Ca^{2-3\gamma} - Da^{2-2n}\right]\chi_\omega(a) = 0,$$

where

$$A = \frac{9\pi^2 c^4 R_0^6}{4\hbar^2 G_0^2}\frac{\Omega_0 H_0^2}{1-n},$$
$$B = \Upsilon_{\rm cl}\frac{9\pi^2 c^2 R_0^6}{8\hbar^2 G_0^2}\frac{\Omega_0^2 H_0^4}{1-n},$$
$$C = \Xi\frac{27\pi^2 c R_0^6}{4\hbar G_0}\frac{\Omega_0 H_0^2}{2n-3},$$
$$D = \frac{9\pi^2 k c^6 R_0^6}{4\hbar^2 G_0^2}. \tag{176}$$

The coefficient D carries the sign of k. Thus, the curvature term should not be interpreted as positive-definite unless the curvature choice has already been fixed.

It is advantageous to remove the first-derivative term by defining

$$\chi_\omega(a) = a^{-q/2}u_\omega(a). \tag{177}$$

The mode equation becomes

$$u_\omega''(a) + V_{\rm eff}(a;\omega)u_\omega(a) = 0, \tag{178}$$

with

$$V_{\rm eff}(a;\omega) = \frac{3c^2\omega^2}{4\pi G_0}a^{-(n+2)} + Aa^{4-n-3\gamma} + Ba^{6-6\gamma} + Ca^{2-3\gamma} - Da^{2-2n} - \frac{q(q-2)}{4a^2}.$$

This is the scalar-clock version of the Schrödinger-like Wheeler–DeWitt equation. Note that the new term's scaling, $a^{-(n+2)}$, is controlled by the same exponent n as the gravitational term. The clock is therefore not an external add-on to the model; it is tied to the scale-dependent gravitational dynamics.

The relational interpretation can also be seen at the classical level. For a free scalar field,

$$\dot\phi = \frac{N}{2\pi^2 R_0^3 a^3}p_\phi, \tag{179}$$

and on a classical branch with $N = 1$, Equation (165) gives

$$\dot a^2 = a^2 F(a) + \frac{G(a)\,p_\phi^2}{3\pi^3 c^2 R_0^6 a^4}, \tag{180}$$

which reduces to $\dot a^2 = a^2 F(a)$ in the $p_\phi = 0$ sector, as shown above. Dividing by $\dot\phi^2$ from Equation (179) gives the *exact* relational trajectory,

$$\left(\frac{da}{d\phi}\right)^2 = \frac{4\pi^4 R_0^6 a^8}{p_\phi^2}F(a) + \frac{4\pi G(a)a^2}{3c^2}. \tag{181}$$

The second term is the backreaction of the clock field's own kinetic energy on the geometry, and it does not vanish on the branch $p_\phi \neq 0$ used to define the clock. Retaining it is necessary in general: dropping it while still requiring $p_\phi \neq 0$ for ϕ to serve as a clock would be inconsistent.

Motivated by the test-field philosophy of Piazza and Vareilles [39], who introduce proper time as an additional minisuperspace degree of freedom and restrict attention to solutions in which it has negligible backreaction on the metric, we work in the regime where the second term of Equation (181) is small compared with the magnitude of the first:

$$\varepsilon(a, p_\phi) \equiv \left| \frac{G(a)\, p_\phi^2}{3\pi^3 c^2 R_0^6\, a^6 F(a)} \right| \ll 1. \tag{182}$$

This is the same ratio that controls Equation (180) itself, so a single condition governs both the gravitational and the relational equations of motion. Under Equation (182), Equation (181) reduces at leading order to

$$\left(\frac{da}{d\phi}\right)^2 \simeq \frac{4\pi^4 R_0^6 a^8}{p_\phi^2} F(a), \tag{183}$$

which is the relation used in the remainder of this section. This relation is, in addition, defined only on the branch $p_\phi \neq 0$, for which ϕ is monotonic in t and can serve as a relational time variable, as noted in the opening paragraph of this section; on the $p_\phi = 0$ sector, ϕ does not evolve and cannot parametrize a trajectory $a(\phi)$ at all.

A structural feature of Equation (182) is that $\varepsilon(a, p_\phi) \to \infty$ as $a \to a_t$, where a_t is defined by $F(a_t) = 0$, for any fixed $p_\phi \neq 0$. The test-field approximation therefore breaks down in a neighborhood of the leading-order turning point, no matter how small the nonzero clock momentum is chosen. The root of $F(a) = 0$ is consequently the turning point of the leading-order test-field trajectory (Equation (183)), but not generally of the exact backreacting dynamics (Equation (181)). Determining the exact turning point in the presence of clock backreaction would require retaining the second term in Equation (181), which we do not attempt here.

This breakdown is consistent with the broadening of the wave packet near a_t, shown in Figure 8: both the leading-order classical trajectory and the test-field approximation used to derive it cease to provide a controlled description in that region. Ref. [39] provides a more complete test-field treatment in which evolution through the bounce region is analyzed explicitly. We make no corresponding claim about the exact trajectory at or beyond a_t; the present construction is restricted to the regime (Equation (182)) away from the turning point.

5.1. Wave Packets and Classical Recovery

The separated functions $\chi_\omega(a)$ are mode functions. A semiclassical cosmological state should instead be built as a superposition of modes,

$$\Psi(a, \phi) = \int d\omega\, A(\omega) e^{i\omega\phi} \chi_\omega(a), \tag{184}$$

where $A(\omega)$ is sharply peaked around ω_0. The Gaussian packet used below is not a new exact solution of the Wheeler–DeWitt equation, and it does not replace the Bessel, Airy, or WKB solutions discussed earlier. It is a narrow-packet approximation to a superposition of the Wheeler–DeWitt modes, used to describe how a localized state follows a classical trajectory in scalar-field time.

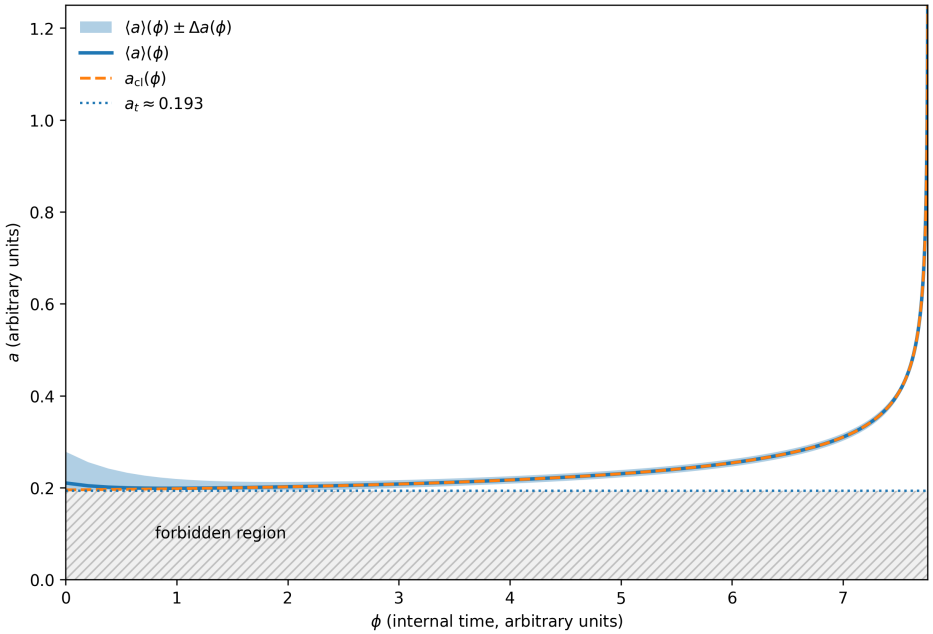


Figure 8. Quantum-to-classical correspondence in scalar-field time for the case $n = 3$, $\gamma = 1$, $q = 1$, $\mathrm{Y}_{\mathrm{cl}} = 0$, and $k = 0$, with $\xi_{\mathrm{QG}} = 122/(15\pi)$ and $\Xi = \xi_{\mathrm{QG}}/R_0^2$. The dashed curve shows the leading-order (test-field) classical relational trajectory $a_{\mathrm{cl}}(\phi)$ obtained from Equation (183), valid subject to the condition in Equation (182). The solid curve shows the expectation value $\langle a\rangle(\phi)$, and the shaded band represents the quantum spread $\Delta a(\phi)$. The horizontal dotted line marks the turning point a_t of this leading-order trajectory, defined by $F(a_t) = 0$; as discussed in Section 5, the test-field approximation itself breaks down near a_t, consistent with the broadening of the quantum spread shown here. The hatched region denotes the classically forbidden sector. The figure illustrates that the state is broad near the turning point but becomes sharply peaked around the classical trajectory at larger scale factors.

In the oscillatory regime, each mode may be written in WKB form as

$$\chi_\omega(a) \simeq \mathcal{A}(a,\omega)e^{iS(a,\omega)}. \tag{185}$$

The phase of the wave packet is then $\omega\phi + S(a,\omega)$. A stationary phase gives

$$\frac{\partial}{\partial\omega}[\omega\phi + S(a,\omega)]_{\omega=\omega_0} = 0, \tag{186}$$

or

$$\phi = -\left.\frac{\partial S(a,\omega)}{\partial\omega}\right|_{\omega=\omega_0}. \tag{187}$$

This relation defines the trajectory followed by the peak of the wave packet. In the large-a semiclassical regime, and for modes satisfying the negligible-backreaction condition in Equation (182), that trajectory agrees with the leading-order classical relational solution determined by Equation (183).

For the illustrative packet diagnostics below, we adopt the factor-ordering measure on a constant-ϕ slice,

$$d\mu(a) = a^q\, da. \tag{188}$$

Therefore, expectation values are defined by

$$\langle f(a)\rangle(\phi) = \frac{\int_0^\infty da\, a^q f(a)|\Psi(a,\phi)|^2}{\int_0^\infty da\, a^q |\Psi(a,\phi)|^2}. \tag{189}$$

In particular,

$$\langle a\rangle(\phi) = \frac{\int_0^\infty da\, a^{q+1}|\Psi(a,\phi)|^2}{\int_0^\infty da\, a^q|\Psi(a,\phi)|^2}, \qquad (\Delta a)^2(\phi) = \langle a^2\rangle - \langle a\rangle^2. \tag{190}$$

A state is semiclassical when

$$\frac{\Delta a}{\langle a\rangle} \ll 1. \tag{191}$$

To see the classical limit explicitly, suppose the probability density is localized around the stationary-phase trajectory $\bar{a}(\phi)$, with $\bar{a}(\phi) = a_{\rm cl}(\phi)$, and is well approximated near its peak by

$$|\Psi(a,\phi)|^2 \simeq \mathcal{N}^2(\phi)\exp\left[-\frac{(a-\bar{a}(\phi))^2}{2\sigma_a^2(\phi)}\right], \qquad \sigma_a(\phi) \ll \bar{a}(\phi). \tag{192}$$

Since the packet is assumed to be localized away from $a = 0$, the lower limit of the Gaussian integral may be extended to $-\infty$ at leading order. With $a = \bar{a} + x$, expansion of the measure gives

$$a^q = \bar{a}^q\left[1 + q\frac{x}{\bar{a}} + \frac{q(q-1)}{2}\frac{x^2}{\bar{a}^2} + \cdots\right]. \tag{193}$$

Using the standard Gaussian moments, one obtains

$$\langle a\rangle(\phi) = \bar{a}(\phi)\left[1 + q\frac{\sigma_a^2(\phi)}{\bar{a}^2(\phi)} + \mathcal{O}\left(\frac{\sigma_a^4}{\bar{a}^4}\right)\right], \tag{194}$$

and

$$(\Delta a)^2(\phi) = \sigma_a^2(\phi) + \mathcal{O}\left(\frac{\sigma_a^4}{\bar{a}^2}\right). \tag{195}$$

Thus, to leading order,

$$\langle a\rangle(\phi) \simeq a_{\rm cl}(\phi), \qquad \frac{\Delta a}{\langle a\rangle} \simeq \frac{\sigma_a}{\bar{a}}. \tag{196}$$

For the representative choice $q = 1$, this reduces to

$$\langle a\rangle \simeq \bar{a} + \frac{\sigma_a^2}{\bar{a}}, \qquad (\Delta a)^2 \simeq \sigma_a^2. \tag{197}$$

The measure-induced shift of the packet center is therefore negligible whenever $\sigma_a/\bar{a} \ll 1$. Classical recovery fails near a turning point or near the small-a region, where the packet broadens and the quantum terms are no longer small.

5.2. Hamilton–Jacobi Limit and Probability Current

The same result follows from the Hamilton–Jacobi form of the Wheeler–DeWitt equation. Write

$$\Psi(a,\phi) = R(a,\phi)e^{iS(a,\phi)/\hbar}. \tag{198}$$

Substitution into Equation (169) and taking the real part gives

$$-(\partial_a S)^2 + \frac{3c^2}{4\pi G(a)a^2}(\partial_\phi S)^2 + \frac{9\pi^2c^4R_0^6}{4G(a)^2}a^4F(a) + Q_\hbar(a,\phi) = 0, \tag{199}$$

where

$$Q_\hbar = \frac{\hbar^2}{R}\left[\partial_a^2 R + \frac{q}{a}\partial_a R - \frac{3c^2}{4\pi G(a)a^2}\partial_\phi^2 R\right]. \tag{200}$$

When $Q_\hbar$ is negligible, Equation (199) reduces to the classical Hamilton–Jacobi equation associated with Equation (165). This is the precise sense in which the modified Friedmann dynamics are recovered from the Wheeler–DeWitt phase in the large-scale, oscillatory regime. The resulting Hamilton–Jacobi equation corresponds to the full backreacting scalar–gravity system and therefore reproduces the exact relational equation (181). The reduced trajectory (183) follows only after the additional test-field condition (182) is imposed.

The two-variable Wheeler–DeWitt equation also admits a conserved minisuperspace current. Multiplying Equation (169) by a^q and using the fact that the coefficients are real gives

$$\partial_a J_a + \partial_\phi J_\phi = 0, \tag{201}$$

with

$$J_a = \frac{a^q}{2i}(\Psi^* \partial_a \Psi - \Psi \partial_a \Psi^*) \tag{202}$$

and

$$J_\phi = -\frac{3c^2 a^q}{8\pi G(a) a^2 i}(\Psi^* \partial_\phi \Psi - \Psi \partial_\phi \Psi^*). \tag{203}$$

This generalizes the one-dimensional current used in Section 4. In the WKB regime, the sign of J_a separates outgoing and incoming branches, while J_ϕ describes the flow with respect to the scalar-field clock [5].

5.3. Interpretation of the Scalar-Clock Figure

Figure 8 summarizes the scalar-clock interpretation. The dashed curve is the leading-order test-field relational trajectory obtained from Equation (183), using the same modified Friedmann function $F(a)$ that enters the Wheeler–DeWitt equation. The solid curve and shaded band show the expectation value and spread of a narrow quantum packet. Near the turning point, the packet is broad and the classical trajectory is not a good description of the state. At larger scale factors, the packet narrows relative to its mean value, and $\langle a \rangle(\phi)$ follows $a_{\rm cl}(\phi)$. This illustrates the expected semiclassical localization within the narrow-packet approximation.

The scalar field does not create a new Friedmann model; rather, it provides the Wheeler–DeWitt wave function with a relational time variable. In the leading-order test-field description, a finite root of $F(a)$ appears in both the approximate classical relational trajectory and the quantum mode structure. The exact backreacting dynamics of Equation (181), however, need not possess a turning point at the same value of a.

In the large-a oscillatory regime, subject to Equation (182), the WKB phase, conserved current, and expectation value of a narrow packet give the same semiclassical picture: the quantum state becomes peaked around the leading-order modified Friedmann trajectory. Near the turning-point and small-a regions, the packet broadens, the test-field approximation ceases to be controlled, and the quantum terms can no longer be neglected. The classical description is therefore inadequate in that regime.

6. Discussion

Allowing the gravitational coupling to depend on the scale factor modifies the first integral of the Newtonian equation of motion through the effective couplings $G^*(a)$, $G_1^{*2}(a)$, and $G_2^{*2}(a)$. Because these terms scale differently with a, the running reorganizes the small-scale structure of the modified Friedmann equation rather than simply rescaling Newton's constant.

For the power-law ansatz $G(a) = G_0 a^n$, this reorganization is controlled entirely by the exponent n. In the dust, flat, $\Upsilon_{\rm cl} = 0$ case, the matter and quantum-correction terms scale as a^{n-3} and a^{2n-5}, respectively. These exponents coincide at $n = 2$, where the two

terms lock onto the same power of a and no isolated turning point can exist. For $n > 2$, the matter term is the more singular contribution near $a = 0$ and carries a negative coefficient, so $H^2(a) < 0$ there, while the quantum-correction term restores $H^2 > 0$ at larger a. The root separating these regions is a genuine bounce. For $3/2 < n < 2$, the quantum term dominates but its coefficient is positive, so the small-a region remains classically allowed; any root in this window is a recollapse scale, not a bounce. The boundary $n = 3/2$ marks the sign change of the quantum-correction coefficient.

A zero of $H^2(a)$ is therefore not sufficient for singularity avoidance. A true bounce requires the additional sign condition: $H^2 < 0$ below the root and $H^2 > 0$ above it. Without this check, a formal turning point may be misidentified. Every root in the parameter survey of Section 2.8 is classified on this basis.

The Wheeler–DeWitt analysis provides the corresponding minisuperspace description of this effective model. The running of $G(a)$ enters the minisuperspace potential explicitly, and the resulting wave functions reflect the sign structure of the modified Friedmann equation. For the dust case with $n = 2$, the equation reduces to a Bessel problem. With the ordering $q = 3/4$, the regular solution satisfies the DeWitt condition $\psi(0) = 0$; with $q = 1$, it is proportional to J_0 and remains finite but nonzero at the origin. DeWitt suppression and regular finite behavior at $a = 0$ are physically distinct. The factor-ordering parameter controls which case applies, while the scale-dependent potential determines the structure of the Wheeler–DeWitt equation itself.

The Airy and radiation-era examples extend this picture beyond Bessel sectors. Their significance is not that they add new qualitative behavior but that they confirm the same three possibilities—DeWitt suppression, regularity, oscillatory large-a behavior—within different matter and running-exponent combinations, all from the same potential structure.

The WKB analysis sharpens the semiclassical reading. For the values of $\gamma = 1$, $n = 3$, $q = 1$, $k = \mathrm{Y}_{\mathrm{cl}} = 0$, the reduced Wheeler–DeWitt equation has a single turning point at $a_t \simeq 0.193$ (in the arbitrary units of Equation (128)). The WKB solution is exponentially suppressed for $a < a_t$ and oscillatory for $a > a_t$. The conserved probability current then distinguishes the two oscillatory branches: the outgoing branch carries positive flux, the incoming branch negative flux, and a real standing-wave carries none. Oscillatory behavior alone does not select a direction of semiclassical evolution; the current does.

The scalar-field clock ties these threads together relationally. In the two-dimensional Wheeler–DeWitt equation (Equation (169)), the clock term scales as $a^{-(n+2)}$, so the same exponent governing the running of $G(a)$ also controls the small-a behavior of the relational dynamics. The relational comparison is restricted to the test-field regime defined by Equation (182), in which the clock kinetic energy has negligible backreaction on the scale-factor dynamics. This approximation necessarily breaks down near the leading-order root $F(a_t) = 0$, so the present analysis does not determine the exact backreacting trajectory through the turning-point region.

The scope of this model is limited. It is an effective, homogeneous, isotropic minisuperspace model derived from a quantum-corrected Newtonian cosmology. This construction should therefore be interpreted as an effective minisuperspace quantization motivated by modified Friedmann dynamics rather than as a derivation from the full Einstein–Hilbert action. It does not address anisotropies, inhomogeneous perturbations, or the full constraint algebra of general relativity. The dimensionless coefficient $\xi_{\mathrm{QG}} = 122/(15\pi)$ is fixed by the adopted one-loop potential, whereas the effective cosmological coefficient $\Xi = \xi_{\mathrm{QG}}/R_0^2$ depends on the reference scale introduced in the Newtonian construction. The normalized combination $\zeta = \hbar G_0 \Xi / c^3$ is therefore used only in dimensionless parameter surveys. The power law $G(a) = G_0 a^n$ is a local early-time scaling ansatz; any complete model must account for the transition to the observed, effectively constant G at late times, as sketched in

Section 2.7. The model instead provides a simplified minisuperspace framework in which the consequences of a running gravitational coupling can be tracked through the modified Friedmann equation to the Wheeler–DeWitt potential and semiclassical limit.

7. Conclusions

Starting from a Newtonian cosmological construction inspired by a corrected two-body gravitational potential and a scale-dependent gravitational coupling, we derived an effective Friedmann-type equation and a corresponding Wheeler–DeWitt-type equation in which the running of $G(a)$ changes the small-a structure of both the classical and quantum dynamics. For the power-law form $G(a) = G_0 a^n$, the dust, flat, $\Upsilon_{\rm cl} = 0$ model develops two natural analytic boundaries at $n = 3/2$ and $n = 2$, separating regimes with qualitatively different turning-point and singularity structures.

Minisuperspace quantization leads to a Wheeler–DeWitt equation whose effective potential is determined by the same scale-dependent structure. Exact Bessel and Airy solutions, together with a numerical radiation-era example, exhibit three distinct behaviors near $a = 0$: DeWitt suppression ($\psi(0) = 0$), regularity without suppression ($\psi(0) \neq 0$), and oscillatory semiclassical behavior at large a. The factor-ordering parameter controls which of the first two applies; the model separates these cases, rather than conflating regularity with singularity avoidance.

The WKB analysis for the representative model ($n = 3$, $\gamma = 1$, $q = 1$) gives a forbidden small-a region, a single turning point, and an oscillatory large-a branch. The conserved probability current distinguishes expanding and contracting semiclassical branches, while the Hamilton–Jacobi limit recovers the modified Friedmann dynamics as the leading-order phase of the wave function. Treating a homogeneous scalar field as a weakly backreacting internal clock, wave packets can be constructed and followed in relational time. Away from the turning-point region and within the test-field regime of Equation (182), the packets narrow onto the leading-order classical relational trajectory at larger-a. The clock term inherits the same running exponent n, coupling the timekeeping structure directly to the scale-dependent gravitational dynamics.

In the early-universe scaling regime considered here, the running of $G(a)$ is not just a perturbative correction. This term changes the qualitative structure of both the classical and quantum cosmological equations, and the same scale dependence appears consistently across the Friedmann dynamics, Wheeler–DeWitt potential, WKB turning point, and scalar-clock semiclassical limit.

Several extensions are needed to determine whether this mechanism survives contact with observations. The full dimensional parameter space $(n, \gamma, \Xi, \Upsilon_{\rm cl}, q)$, or, equivalently, the normalized survey space $(n, \gamma, \zeta, \Upsilon_{\rm cl}, q)$, should be mapped systematically, with the Type I/II/III classification applied throughout and the pure power law replaced by a transition profile, such as Equation (51), and matched to observational bounds. The phenomenological consequences of the running—its effect on the BBN expansion rate, the growth of linear matter perturbations, and the CMB acoustic scale—are examined in the companion paper [34]. The present analysis therefore treats the power law as an early-universe scaling limit rather than as a global description of gravity.

Author Contributions: Conceptualization, J.A.S. and J.M.C.; methodology, J.A.S. and J.M.C.; software, R.B., B.R.F. and I.J.; validation, R.B., B.R.F., I.J., J.A.S. and J.M.C.; formal analysis, R.B., B.R.F. and I.J.; investigation, J.A.S. and J.M.C.; resources, J.A.S. and J.M.C.; writing—original draft preparation, J.A.S. and J.M.C.; writing—review and editing, J.A.S. and J.M.C.; visualization, R.B., B.R.F., I.J., J.A.S. and J.M.C.; supervision, J.A.S. and J.M.C.; project administration, J.A.S. and J.M.C. All authors have read and agreed to the published version of the manuscript.

Funding: This research received no external funding.

Data Availability Statement: No new data were created or analyzed in this study. Data sharing is not applicable to this article.

Conflicts of Interest: The authors declare no conflicts of interest.

Abbreviations

The following abbreviations are used in this manuscript:

WDW	Wheeler–DeWitt
WKB	Wentzel–Kramers–Brillouin
FRW	Friedmann–Robertson–Walker
QC	Quantum cosmology
SDG	Scale-dependent gravity
EOS	Equation of state
a	Cosmological scale factor
R	Physical radius of the Newtonian sphere
R_0	Comoving reference radius
H	Hubble parameter
$G(a)$	Scale-dependent gravitational coupling
$G^*(a)$	Effective gravitational coupling appearing in the matter term
$G_1^{*2}(a)$	Effective coupling associated with the classical correction term
$G_2^{*2}(a)$	Effective coupling associated with the quantum correction term
ρ	Mass density
ρ_0	Present-day mass density
γ	Barotropic index in the equation of state
k	Spatial curvature parameter
$\Upsilon_{\rm cl}$	Effective coefficient of the higher-order classical correction
$\xi_{\rm QG}$	Dimensionless one-loop coefficient in the quantum-corrected Newtonian potential
Ξ	Dimensionful cosmological quantum-correction coefficient, $\Xi = \xi_{\rm QG}/R_0^2$
ζ	Dimensionless normalized quantum-correction parameter, $\zeta = \hbar G_0 \Xi / c^3$
q	Factor-ordering parameter
$\psi(a)$	Wheeler–DeWitt wave function
ϕ	Scalar-field internal clock
$J(a)$	Minisuperspace probability current

References

1. Penrose, R. Gravitational collapse and space-time singularities. *Phys. Rev. Lett.* **1965**, *14*, 57–59. [CrossRef]
2. Hawking, S.W.; Ellis, G.F.R. *The Large Scale Structure of Space-Time*; Cambridge Monographs on Mathematical Physics; Cambridge University Press: Cambridge, UK, 1973.
3. DeWitt, B.S. Quantum theory of gravity. I. The canonical theory. *Phys. Rev.* **1967**, *160*, 1113–1148. [CrossRef]
4. Hartle, J.B.; Hawking, S.W. Wave function of the Universe. *Phys. Rev. D* **1983**, *28*, 2960–2975. [CrossRef]
5. Vilenkin, A. Boundary conditions in quantum cosmology. *Phys. Rev. D* **1986**, *33*, 3560–3569. [CrossRef] [PubMed]
6. Bojowald, M. Absence of a singularity in loop quantum cosmology. *Phys. Rev. Lett.* **2001**, *86*, 5227–5230. [CrossRef] [PubMed]
7. Ashtekar, A.; Pawlowski, T.; Singh, P. Quantum nature of the Big Bang. *Phys. Rev. Lett.* **2006**, *96*, 141301. [CrossRef] [PubMed]
8. Khoury, J.; Ovrut, B.A.; Steinhardt, P.J.; Turok, N. Ekpyrotic universe: Colliding branes and the origin of the hot Big Bang. *Phys. Rev. D* **2001**, *64*, 123522. [CrossRef]
9. Gielen, S.; Magueijo, J. Quantum analysis of the recent cosmological bounce in the comoving Hubble length. *Phys. Rev. D* **2023**, *107*, 023518. [CrossRef]
10. Gouba, L. Quantum Newtonian cosmology revisited. *Lett. High Energy Phys.* **2022**, *5*, 321. [CrossRef]
11. Leszczyńska, K. Quantum cosmology and varying physical constants. *Universe* **2017**, *3*, 46. [CrossRef]
12. Donoghue, J.F. Leading quantum correction to the Newtonian potential. *Phys. Rev. Lett.* **1994**, *72*, 2996–2999. [CrossRef] [PubMed]
13. Bargueño, P.; Bravo Medina, S.; Nowakowski, M.; Batic, D. Newtonian cosmology with a quantum bounce. *Eur. Phys. J. C* **2016**, *76*, 543. [CrossRef]

14. Halliwell, J.J. Derivation of the Wheeler–DeWitt equation from a path integral for minisuperspace models. *Phys. Rev. D* **1988**, *38*, 2468–2481. [CrossRef] [PubMed]
15. Senjaya, D. Exact solution to the Wheeler–DeWitt equation: Early and current Universe. *J. High Energy Astrophys.* **2024**, *44*, 494–499. [CrossRef]
16. Bodmann, B.; Hadjimichef, D.; Hess, P.O.; de Freitas Pacheco, J.; Weber, F.; Razeira, M.; Degrazia, G.A.; Marzola, M.; Vasconcellos, C.A.Z. A Wheeler–DeWitt non-commutative quantum approach to the branch-cut gravity. *Universe* **2023**, *9*, 428. [CrossRef]
17. Kiefer, C.; Peter, P. Time in quantum cosmology. *Universe* **2022**, *8*, 36. [CrossRef]
18. Hamber, H.W.; Liu, S. On the quantum corrections to the Newtonian potential. *Phys. Lett. B* **1995**, *357*, 51–56. [CrossRef]
19. Casadio, R.; Giugno, A.; Giusti, A.; Lenzi, M. Quantum corpuscular corrections to the Newtonian potential. *Phys. Rev. D* **2017**, *96*, 044010. [CrossRef]
20. Scardigli, F.; Lambiase, G.; Vagenas, E.C. GUP parameter from quantum corrections to the Newtonian potential. *Phys. Lett. B* **2017**, *767*, 242–246. [CrossRef]
21. Mandal, R.; Gangopadhyay, S.; Lahiri, A. Newtonian cosmology from quantum corrected Newtonian potential. *Phys. Lett. B* **2023**, *839*, 137807. [CrossRef]
22. Hanımeli, E.T.; Tutusaus, I.; Lamine, B.; Blanchard, A. Low-redshift tests of Newtonian cosmologies with a time-varying gravitational constant. *Mon. Not. R. Astron. Soc.* **2020**, *497*, 4407–4415. [CrossRef]
23. Barrow, J.D. Time-varying *G*. *Mon. Not. R. Astron. Soc.* **1996**, *282*, 1397–1406. [CrossRef]
24. Bjerrum-Bohr, N.E.J.; Donoghue, J.F.; Holstein, B.R. Quantum gravitational corrections to the nonrelativistic scattering potential of two masses. *Phys. Rev. D* **2003**, *67*, 084033. Erratum in *Phys. Rev. D* **2005**, *71*, 069903. [CrossRef]
25. Kirilin, G.G. Quantum corrections to the Schwarzschild metric and reparametrization transformations. *Phys. Rev. D* **2007**, *75*, 108501. [CrossRef]
26. Donoghue, J.F. The effective field theory treatment of quantum gravity. *AIP Conf. Proc.* **2012**, *1483*, 73–94. [CrossRef]
27. Codello, A.; Jain, R.K. On the covariant formalism of the effective field theory of gravity and leading order corrections. *Class. Quantum Grav.* **2016**, *33*, 225006. [CrossRef]
28. Codello, A.; Jain, R.K. On the covariant formalism of the effective field theory of gravity and its cosmological implications. *Class. Quantum Grav.* **2017**, *34*, 035015. [CrossRef]
29. Donoghue, J.F.; El-Menoufi, B.K. Nonlocal quantum effects in cosmology: Quantum memory, nonlocal FLRW equations, and singularity avoidance. *Phys. Rev. D* **2014**, *89*, 104062. [CrossRef]
30. Reuter, M. Nonperturbative evolution equation for quantum gravity. *Phys. Rev. D* **1998**, *57*, 971–985. [CrossRef]
31. Bonanno, A.; Saueressig, F. Asymptotically safe cosmology—A status report. *Comptes Rendus Phys.* **2017**, *18*, 254–264. [CrossRef]
32. Faraoni, V. *Cosmology in Scalar–Tensor Gravity*; Kluwer Academic Publishers: Dordrecht, The Netherlands, 2004.
33. Overduin, J.M.; Wesson, P.S. Kaluza–Klein gravity. *Phys. Rep.* **1997**, *283*, 303–378. [CrossRef]
34. Furst, B.R.; Jarra, I.; Bolle, R.; Conroy, J.M.; Secrest, J.A. Scale-Dependent Gravity in Quantum Cosmology II: Phenomenological Consistency Tests from BBN, Structure Growth, and the CMB. *Astron. Astrophys.* **2026**, *in preparation*. [CrossRef]
35. Atkatz, D. Quantum cosmology for pedestrians. *Am. J. Phys.* **1994**, *62*, 619–627. [CrossRef]
36. Bender, C.M.; Orszag, S.A. *Advanced Mathematical Methods for Scientists and Engineers*; McGraw-Hill: New York, NY, USA, 1978.
37. Fröman, N.; Fröman, P.O. *JWKB Approximation: Contributions to the Theory*; North-Holland: Amsterdam, The Netherlands, 1965.
38. Monerat, G.A.; Santos, C.G.M.; Alvarenga, F.G.; Gonçalves, S.V.B.; Fracalossi, R.; Corrêa Silva, E.V.; Oliveira-Neto, G. Quantum cosmology with many fluids and the choice of cosmological time. *Braz. J. Phys.* **2020**, *50*, 89–104. [CrossRef]
39. Piazza, F.; Vareilles, S. Time as a test-field: The no-boundary universe in motion and a smooth radiation bounce. *Class. Quantum Grav.* **2026**, *43*, 055007. [CrossRef]

Disclaimer/Publisher's Note: The statements, opinions and data contained in all publications are solely those of the individual author(s) and contributor(s) and not of MDPI and/or the editor(s). MDPI and/or the editor(s) disclaim responsibility for any injury to people or property resulting from any ideas, methods, instructions or products referred to in the content.